I love that dirty water? Value of water quality in recreation sites

Christopher R. Knittel, Jing Li, Xibo Wan[1]

JOB MARKET PAPER

First Version: Nov 27th, 2022

This Version: December 26, 2022 (Latest Version: Here)

ABSTRACT

Analyses of policies that improve water quality often suggest that the costs far exceed the benefits. Keiser and Shapiro (2019a) suggests that this partially arises from the difficulty of accurately measuring the benefits. Measuring these benefits is often complicated by the lack of data on visitations. In this paper, we study the value of recreation amenities nationwide using data from mobile devices about aggregate visitor counts and dwell time at each water recreation site by home census block group. We combine the mobile movement data with data on water quality and weather to construct a comprehensive, novel, and detailed dataset of around 32k water-based recreational sites with linkage to recreation visits made by 23 million representative residents. Using these data, we construct aggregate share data of recreation visits from each census block group to each site. We develop a random coefficient logit model of site choice to estimate the welfare effects of water quality improvements in the US. Our results suggest recreators are willing to pay an average of $2.55 for a 1-meter increase in Secchi depth in the sites they visited, ranging from $1.3 to $2.2 across census regions. Our work suggests that the benefits of improving the water quality of all sites to the level of the cleanest site are $433.26 million. The annual welfare losses due to the most popular and polluted site closure are $2.7 billion and $878.37 million, respectively. Revisiting the water quality changes from 1972 to 2001, Our findings add 1.7% to the previously estimated benefits gained from the Clean Water Act.

KEYWORDS

Water Quality, Recreational Demand, Cell Phone Data, Non-market Valuation

[1]*Christopher R. Knittel:* MIT Sloan School of Management, MIT Center for Energy and Environmental Policy Research, and NBER, knittel@mit.edu. *Jing Li:* MIT Sloan School of Management, lijing@mit.edu. *Xibo Wan* (*Job Market Paper*)*:* MIT Center for Energy and Environment Policy Research, Corresponding author at xwan@mit.edu. We have benefited from conversations with David Keiser, Matt Woerman, Jamie Mullins, Konstantinos Metaxoglou, and various seminar participants at UMass Amherst and the Heartland Environmental and Resource Economics Workshop at Illinois. The views expressed herein are solely those of the authors and are not necessarily those of SafeGraph.

1 INTRODUCTION

In 1995, the Charles River earned a D grade for water quality at its mouth in Boston Harbor, a result of uncontrolled human sewage, industrial waste, and landfills that crept up right to the water's edge. The river was so polluted at the time that the locals joked about people needing tetanus shots if they fell in. The Standells, an American rock band, wrote a song as a mock paean to the city of Boston, Massachusetts, and its then-famously polluted Boston Harbor and Charles River:

"... Yeah, down by the river
Down by the banks of the river Charles
Aw, that's what's happenin', baby
That's where you'll find me
Along with lovers, muggers, and thieves
Aw, but they're cool, too
Well, I love that dirty water
Oh, Boston, you're my home ..."

Due to the ambitious effort made by Environmental Protection Agency (EPA), numerous federal, state, and local agencies as well as nonprofit groups, private institutions, and citizens the Charles River is now both fishable and swimmable. However, reducing water pollution is still a major focus of policy makers. Although the United States has spent approximately $5 trillion to clean up surface water pollution and provide clean drinking water, over half of the US rivers and lakes violate environmental standards.

One puzzle arising from these large investments is that 67 percent of surface water regulations failed a benefit-cost test (Keiser and Shapiro (2019b)). This raises a key question for policy makers as to whether the failure of cost-benefit tests arises because of a downward bias from the true value of surface water quality. As the United States continues putting efforts to clean up surface water pollution, it is critically important to develop a more comprehensive understanding of water quality benefits and to justify the investments. One potential source of a downward bias in benefits is the difficulty in accurately measuring the recreational benefits of clean water. Improvements in water quality increase the utility of using such recreational activities of swimming, boating, and fishing. However, these benefits may be more difficult to quantify that the health benefits from, say, improvements in air quality for a variety of reasons.

In this paper, we ask what are the *nationwide* recreational benefits of surface water quality improvements?

An accurate answer to this question has so far proven elusive for three related reasons. First, it has been difficult to link individual recreation behavior to surface water quality for the entire nation over time. Past research relies on self-report data using on-site surveys or off-site sampling, which often generate localized estimates and often fail to transfer benefits to larger regions (Loomis et al. (1995); Rolfe et al. (2015); Rosenberger and Loomis (2017)). Second, the survey data used for recreation demand studies often suffer from selection biases and recall errors (Connelly and Brown (2011); Dillman (2017); Rylander et al. (1995); Tarrant et al. (1993)). Third, the individual choice sets may be endogenous. Without knowing the actual visits, it is difficult to identify what recreators consider to be the relevant substitutes, and simply specifying the choices could produce significantly larger losses for policies that restrict site access (Parsons et al. (2021); Parsons and Hauber (1998); Parsons et al. (2000)).[2]

To address these challenges, we begin by constructing comprehensive data on recreation visits, water quality, and weather in the lower 48 states from 2018 to 2021. To overcome the difficulty of measuring which sites households visit, as well as the set of potential sites they could visit, we collect from Safegraph which tracks location data from mobile devices. These data measure where a mobile-devise user lives and which water sites they visit. The data allow us to measure each water-based recreation site visit by home census block group (CBG) making it possible to observe the actual linkages between recreation behavior and surface water quality nationwide. We then develop a structural model of site choices to estimate recreation demand for these water-based recreation sites and how this demand is affected by changes in water quality. We include site fixed effects to account for time-invariant differences in the utility of each site and CBG fixed effects to capture unobserved demographic variables that influence the demand for outdoor recreation. In addition, we employ a set of instruments to address the potential omitted variables bias and endogeneity issues. Given our utility parameter estimates, we can measure the welfare impacts of both non-marginal changes in water quality and site closures.

Our data on water quality suggest that despite the large investments in improving water quality, average water quality across all of our recreation sites changed little from 2018. One measure of water quality frequently used is the Secchi depth. The Secchi depth is the depth at which point a Secchi disk, an 8-inch black and white disk, is no longer visible by the naked eye. In our data, the within-site change in annual average Secchi depth from 2018 to 2021 varies from -2.87 meters to 5.15 meters. We also observe large variations in the annual changes in the Secchi depth within a given site. Our empirical strategy will leverage these within-site changes in water quality.

[2]In the following sections, we use recreation visitors and recreators interchangeably.

Our analysis proceeds in three steps. In the first step, we introduce the data that we assemble for this research and the empirical context. The major data for recreation visits is obtained from the Safegraph cell phone database. We match the recreation site polygons with water bodies and flow line layers from National Hydrography Data (NDH) to identify water-based recreation sites[3]. We then match our recreation data to water-quality data from EPA's Water Quality Portal and annual weather data from the PRISM Climate Group. This source provides data on over 23 million households' recreational decisions and residential locations at the CBG level. We focus on the recreation patterns between 2018 and 2021, for which we observe the number of visitors traveling from their home CBG to water-based recreation sites[4]. During this period, people from 216k CBGs visited about 32k water-based recreation sites, where the average number of visits per year is 6,312 and the average number of visitors per year is 2,829.

With these rich data on visitations and water quality, we construct aggregate data on actual site choices for each CBG from 2018 to 2021 and the costs associated with visiting each site from a home CBG. We calculate the travel costs by summing up the out-of-pocket travel costs and the value of travel time for the trip to and from the site. We calculate the travel distance and travel time for each route through the Open Source Routing Machine. We calculate out-of-pocket expenses using state-monthly average gasoline cost data obtained from AAA website[5]. For the value of time, we use the average implied hourly wage of each CBG.

We focus on car-mode trips. We define car-mode trip as any trips traveled within a 300-mile distance based on our travel distance distribution[6]. To determine the market share of recreation trips for each site from a CBG, we define the total market size of water-based recreation by multiplying the average annual number of the device at a CBG by the number of holidays and weekends over a year (115 days). Finally, we match the data with annual precipitation and average temperature from the PRISM Climate Group to control for the impact of weather conditions on recreation trips.

In the second step, we develop a structural model of site choices across time and space to estimate the recreation demand function. Specifically, we cast the water-quality measures as lake characteristics in the static, discrete-choice framework of Berry et al. (1995). We calculate the "market" share of each recreation site within 300 miles from people living in each CBG, specifying the utility of visiting each site to be a

[3]We define "water-based recreation" broadly to include all recreation sites that provide water-related services to humans, such as boating, swimming, or fishing.

[4]The duration of the visit must last at least 4 minutes to count as a visit to a given POI.

[5]We assume the MPG of the average passenger vehicle is 23.3 miles per gallon. The fuel costs per mile for an average passenger vehicle are calculated by multiplying the average gas costs by the MPG for an average vehicle.

[6]Consistent with what we find, the 2017 National Household Travel Survey shows a similar cutoff for car-mode trips. See more details in **Online Appendix A.3**.

function of both water quality the travel costs associated with visiting a given site, and annual weather conditions. Given the richness of our data, we can control for the time-invariant quality of each site by including site fixed effects. As a result, our model relies on temporal variation of water quality measures to explore the impact of water quality on recreation demand. To account for potential endogeneity concerns with respect to travel costs arising through time series changes in gasoline prices, we collect the annual crude oil prices from 2018 to 2021 from US Energy Information Administration (EIA), as the oil prices are plausibly exogenous cost shifters to recreators. We use the interaction between oil price and state dummies, and travel distance as instruments of travel costs. Moreover, we conduct a battery of additional robustness checks that demonstrate that our results are robust to alternative site polygon buffers, market sizes, car-mode trip cutoffs, travel cost definitions, and functional forms.

In the third step, we use our estimated utility parameters to quantify the welfare effects under three water quality scenarios. First, we assess the recreation welfare benefits from water quality improvements by simulating the compensating variation for all the recreation sites experiencing improvements in water quality to the level of the cleanest lake observed in the data. Next, the eutrophication of water bodies has been considered one of the most significant environmental concerns in water-based recreation. It harms human health, contributing to the spread of gastrointestinal and dermatological diseases. We calculate the welfare changes under a site closure scenario that are most likely to be considered by local authorities: closing the recreation sites with eutrophication. Lastly, in response to the COVID-19 pandemic, many popular recreation sites have been temporarily closed. Therefore, we consider closing the most popular recreation destinations as a counterfactual to understand the welfare effects of this policy.

Our results suggest that water quality is likely a strong driver of recreation behavior and welfare changes over our study period. Recreators are willing to pay an average of $2.55 for a 1-meter increase in Secchi depth in the sites they visited. Furthermore, we find some evidence of spatial heterogeneity in water quality preference such that the MWTP for Secchi depth varies from $1.3 to $2.2 across census regions. The three water quality scenarios we discuss above lead to a significant willingness to pay for water quality improvements and for avoiding site closure. We find the benefits from improving the water quality of all sites to the level of the cleanest site is $433.26 million, with spatial heterogeneity across census regions ranging from $50.7 million to $ 100.4 million. Additionally, the welfare losses due to the most popular and polluted site closure are $2.7 billion and $878.37 million, respectively. Revisiting the water quality changes from 1972 to 2001, Our findings add 1.7% to the previously estimated benefits gained from the Clean Water Act.

Our work complements a broad literature that examines the impact of water quality on recreation demand. Most recreation demand studies use surveys with revealed preference and stated preference methods to estimate benefits from water quality improvements, however, these studies are often geographically and temporally limited (Egan et al. (2009); Fenichel et al. (2013); Hushak et al. (1988); Hynes et al. (2013); Keiser and Shapiro (2019b); Kelch et al. (2006); Lupi et al. (2003); Melstrom and Lupi (2013); Phaneuf and Smith (2005); Provencher and Bishop (1997); Van Houtven et al. (2014); Viscusi et al. (2008); Whitehead et al. (2010)). For example, Dundas and von Haefen (2020) uses one of the largest recreation data sets, the NOAA's Marine Recreational Information Program (MRIP) data, to examine the effects of weather on the shoreline marine recreational fishing demand. While they find the extreme heat significantly reduces recreation participation across 17 states, their study area is mainly located in the Atlantic and Gulf Coast regions. Relative to these papers, we use the largest recreation data sets currently available, utilizing cell phone data from nearly 23 million residents and water quality data across the lower 48 US states. To the best of our knowledge, our paper provides the first national estimates of recreation demand on water quality in water-based recreation sites.

We are not the first to use cell phone data, however. This paper contributes to a growing literature on recreation demand using innovative data. A recent set of papers highlight the potential promise of innovative data acquisition efforts such as cell phone records (Kubo et al. (2020); Merrill et al. (2020); Newbold et al. (2022)) and mining of social media data (Ghermandi (2018); Keeler et al. (2015); Sinclair et al. (2018); Sonter et al. (2016); Spalding et al. (2017); White et al. (2022); Wood et al. (2020)). For example, Merrill et al. (2020) combines the cell phone data with on-the-ground observations of visitation to water recreation areas in New England, and then fits a model to estimate daily visitation for four months to more than 500 sites. Newbold et al. (2022) utilizes remote sensing satellite data and cell phone data to estimate a recreation demand site-choice model of 100 lakes in California. By using simulated data in a Monte Carlo analysis, they develop an information valuation framework for harmful algal blooms (HABs) and find the total value of a perfect early warning system would have been $2.46 million. This paper methodologically differs from prior recreation demand studies (Moeltner and Englin (2004); Morey et al. (1993); Phaneuf et al. (2000); Von Haefen and Phaneuf (2003)) by using a random coefficient logit model to estimate the recreation demand on water quality. Our work also extends prior work in the IO literature by employing a random coefficient logit model in the context of recreation demand.

The rest of this paper proceeds as follows. Section 2 presents the study area and data. Section 3 describes structural models used for estimating the water quality impact on recreation demand. Section 4 provides

results and sensitivity tests. Section 5 examines predicted demand and welfare changes from our non-marginal change and site closure simulations. Section 7 provides a summary of our findings, limitations of our study, and implications for future research.

2 DATA AND SUMMARY STATISTICS

2.1 *Data*

The main data set measuring recreational site visits is taken from the SafeGraph pattern data[7]. These data contain information such as aggregated visitor counts to individual amenities from CBGs as well as the time spent at each site. SafeGraph receives raw GPS data from multiple different mobile app providers on both iOS and Android systems[8]. We restrict our sample from 2018 to 2021 and only focus on points of interest (POIs) within the sub-categories tracking nature park and other similar institutions[9]. Next, we focus on recreation sites whose area size is above 1 Ha (10,000 m^2) and whose annual visits are more than 500. Finally, to track the annual recreation visits from each CBG (origin) to recreation site (destination), we decompose the distribution of home visitors' CBGs for each site at a year-month and then aggregate the number of visitors at a site from a CBG to a given year[10].

Water quality measures from water quality monitors are obtained from EPA's Water Quality Portal, which includes water quality monitoring data collected by the United States Geological Survey (USGS), the Environmental Protection Agency (EPA), and over 400 states, federal, tribal, and local agencies[11]. We consider dissolved oxygen (DO), Secchi depth, and Chlorophyll-a as our water quality measures since they are the three most common measures of water quality in research on water pollution's economic impacts (Keiser and Shapiro (2019a)). Secchi depth and Chlorophyll-a are good indicators of water quality conditions that are noticed by people. DO is critical for fish survival, and water quality that meets the criteria for fish survival also meets the criteria for most other beneficial water uses and is often of good

[7] SafeGraph issues updates to Places once per month. The pattern data used in this paper was collected in November 2021.

[8] It is worth noting that since SafeGraph estimates visits to the site based on smartphone GPS movements, the data do not cover all actual visitors but rather a subset of users that have a smartphone and who have enabled their phone's GPS location feature in various apps. The data could thus be under-representing visitors from demographic groups that have a lower proclivity to own or use a smartphone (e.g., elderly individuals and low-income residents).

[9] Another concern about cell phone data is the potential for location error. The mobile GPS positioning can only achieve an accuracy of roughly 5 meters. When the cell phone device is in dense urban clusters, the app-based GPS positioning might not be able to distinguish whether a user is in one store or another. However, the recreation site POIs are less likely to have such errors as outdoor recreation sites are often not located side by side.

[10] The visitor's home locations are determined by analyzing 6 weeks of data during nighttime hours (between 6 pm and 7 am). SafeGraph requires a sufficient amount of evidence (total data points and distinct days) to assign a home (common nighttime) geohash-7 for the device, which is then mapped to a census block group, census tract, and country of origin. SafeGraph does not report data unless at least 2 visitors are observed from that group. If there are between 2 and 4 visitors this is reported as 4.

[11] See more details in here: https://www.waterqualitydata.us/

ecological status. Based on the imputation performance on water quality data discussed later in this section, we use Secchi depth as our main water quality measure. **Online Appendix B.1** describes details and steps taken to clean the data.

Several other data are used for our analysis. First, spatial data on rivers and lakes are obtained from the National Hydrography Dataset (NHD), an electronic atlas mapping all U.S. surface waters. NHD contains approximately 200 river basins, 2,000 watersheds, 70,000 named rivers, 3.5 million stream and river miles, and 70 million river nodes in the US. We spatially join the NHD waterbody polygon and river flowline layer with recreational visits geometry data to determine water-based recreational sites.

Second, daily average temperature and precipitation data are generated from the parameter-elevation regressions on the independent slopes model (PRISM 2009). The PRISM model divides the contiguous United States into 2.5 × 2.5 mile grids and uses daily weather station data, while also accounting for factors such as elevation and wind direction, to interpolate weather measures for each grid location. The PRISM data are used to control for the impact of weather on recreation trips.

Third, gas cost data are obtained from AAA website[12], which provide daily national gas prices and daily state-level average prices by gas types (regular, mid-grade, premium, and diesel). To calculate the travel costs for each trip in a year, we scrape the daily snapshot of the AAA website from the Wayback machine and aggregate it to the monthly level for each state since 2018. We also use the annual national crude oil price between 2018 and 2021 from U.S. Energy Information Administration (EIA) to address potential endogeneity issues in the recreation demand estimation.

Last but not least, we use the Open Census data from SafeGraph, which has pre-cleaned the Census data and packaged it into easy-to-use files for each year of the American Community Survey, each including over 7500 attributes like income, age, education, etc.[13]. We use the median household income by CBGs and year for travel cost calculation.

Finally, we obtain the COVID-19 daily cases and deaths data from New York Times[14] and county-day level stay-at-home orders data from Centers for Disease Controls and Prevention (CDC)[15]. To control for the impact of pandemic and lockdown on recreation demand, we aggregate the COVID-19 case and death data

[12]see https://gasprices.aaa.com/todays-state-averages/

[13]See https://www.safegraph.com/free-data/open-census-data

[14]The New York Times. (2021). Coronavirus (COVID-19) Data in the United States, see more information in https://github.com/nytimes/COVID-19-datacoronavirus-COVID-19-data-in-the-united-states

[15]See more in: https://data.cdc.gov/Policy-Surveillance/U-S-State-and-Territorial-Stay-At-Home-Orders-Marc/y2iy-8irm/data

to county-year level and create two indicators for a county implemented the stay-at-home order at a year and a county confirmed any COVID-19 case at a year.

2.2 *Spatial Linkages and Data Description*

We link the different data sets described above in three ways. The first involves linking each recreation site to the associated river or lake. To do that, we begin by obtaining a GIS data layer containing recreation site polygons from SafeGraph that represents the location and spatial extent of sites in our sample. We then intersect the recreation site polygon with the waterbody and flowline layers from the National Hydrography Dataset to identify lake-based and river-based recreation site[16]. Appendix Figure A1 provides more details. After doing that, we narrow down our sample to 47,541 recreation sites. The second linkage involves linking recreation sites to weather conditions. We extract the value of weather data to each recreation site location and aggregate it to the annual level.

The third involves matching each water quality monitor to the associated river or lake. We spatially join the station location data collected from EPA Water Quality Portal with the water-based recreation site polygon to identify corresponding water bodies. The water quality measures for a recreation site are then calculated by taking the average of water quality measures within a water body for each year. Keiser and Shapiro (2019a) suggests evidence of disproportionate distribution of sampling frequency across the U.S. due to hydrology design, monitoring network density, and local government decisions. As a result, it has been difficult to obtain continuous annual readings for each water quality monitor. To address this issue, we employ several machine learning techniques (KNN, Mean, Bayesian Ride, Decision Tree, and MICE) under scenarios with three missing patterns (MCAR, MAR, and MNAR) and four missing fractions (20%,40%,60%, and 80%) to imputed this imbalanced water quality data[17]. After comparing the imputation results across different methods, we impute the Dissolved oxygen and Secchi depth using KNN with 4 neighbors and decide to not use the Chlorophyll-a measure due to the poor imputation performance. We then spatial join the adjusted recreation site polygon with monitor locations to measure water quality data for each site. **Online Appendix B.2** provides details of each method and discussions on imputation results.

[16]We visually inspect the intersection between the site polygon and waterbody layer. In some cases, the site polygon only covers the area where the cell phone device is located but not the lake. We manually adjusted polygon outlines to encompass the complete infrastructure for each lake. For example, for small lake sites, we union the recreation site polygon with intersected water bodies. For large lake sites and river sites, we create a 200-meter buffer of recreation site polygon to cover the water bodies adjacent to a given site. A similar study by Merrill et al. (2022) uses a quarter-mile buffer of each shoreline segment to estimate median water clarity over the last five years' summer months. See more details about polygon adjustments in **Online Appendix A.2**

[17]We also consider using 5-year moving average values and satellite image data to impute our water quality measures. One of the issues with the moving average method is it smooths out the variation across different years, which is what we need for water quality identification. Ross et al. (2019) provides some additional satellite estimates of Secchi depth and Chlorophyll-a data. After merging it with our data, we do not find a major increase in water quality observations.

We then calculate the travel costs based on the monetary travel cost and the opportunity cost of time.[18] Specifically, we first estimate the travel distance and duration from the centroid of a census block group to a recreational site using the Open Source Routing Machine (OSRM)[19]. The visitor's opportunity cost of time in a census block group is measured using the common assumption that it is one-third of the wage rate implied by the census block group's average annual income[20]. Under these assumptions, the total travel costs (TC) are the sum of travel and time-related expenses:

$$TC_{ijt} = 2 * (gs_{st} + f_t) * Dist_{ijt} + 2 * \gamma \frac{Medinc_i}{2080} Time_{ijt} \quad (1)$$

where $Dist_{ijt}$ is the one-way distance between the centroid of a CBG and the recreational site; gs_{st} reports the state-level average gas cost at year t; f_t denotes the marginal maintenance cost, repair cost, and depreciation from AAA reports; we assume $\gamma = 1/3$ indicating the share of the value of travel time used to account for the cost of leisure time, and $medinc_i$ is the median annual income in the visitor's CBG. The median income is divided by 2,080, the number of full-time hours potentially worked in a year.

As the visits data from SafeGraph includes all the recreation trips taken by users from a CBG, people might fly to a recreation site if it is too far away from the origin CBG. We would expect that the preference for travel costs in a flight-mode trip could be quite different from the one in a car-mode trip. Furthermore, it would be difficult to measure the monetary costs associated with flying. Therefore, we restrict ourselves to trips that are likely taken by car. Appendix Figure A3 shows the distribution of one-way trip travel distance across census region in our sample. Looking closely at the tail of the distribution, we find most trips are within a 300-mile travel distance. Thus, we consider it a plausible cutoff to distinguish between a car-mode trip and a flight-mode trip. We also find similar evidence in the 2017 National Household Travel Survey. Appendix Figure A4a shows the distribution of one-way trip travel distance for car-mode trips and Appendix Figure A4b shows the distribution of one-way trip travel distance for flight-mode trips. We find most car-mode trips are within 300-mile travel distance, while most flight-mode trips are beyond 300-mile travel distance[21].

[18] This opportunity cost of time must also be factored into travel cost recreational demand models for a more accurate measure of the value of the recreational experience (Palmquist et al. (2010)).

[19] In some cases, the open source routing machine failed to calculate the travel distance and duration. Instead, we calculate the haversine distance between origins and destination and use the ratio of 1.4 to impute the travel distance and travel time based on observed data. Keiser and Shapiro (2019a) also suggests that the mean ratio of the road distance to the great circle distance is 1.4.

[20] Lupi et al. (2020) suggests that using a fraction (i.e., between one-third and one-half) of this "average wage" as the value of travel time is consistent with past precedent in the literature and a small number of recent studies. We also conduct sensitivity analyses using alternative fractions of the average wage in the Appendix.

[21] Dundas and von Haefen (2020) also assume that any site within 300 miles (roughly a 6-hour drive one way) of each origin zip is in the respondent's choice set. The assumption is based on the notion that 300 miles represent the furthest an individual would likely be able to travel for a single day of localized recreation.

After determining the choice sets for each CBG, we calculate the site trip shares in the following steps. First, we use the statistics of CBG-year-month visitors to estimate the total market size for each census block group in a given year. Specifically, we take the average number of visitors at a CBG each year and consider it as the population of the market. Next, we calculate the total market size by multiplying the population by 115 as we assume that people make 115 recreational choices over a year (once for each weekend or holiday)[22]. Finally, the trip share of a single recreational site is then calculated as the ratio of the trips of this site to the total market size. The outside share is the ratio of the difference between the total market size and total recreation trips from CBG to the total market size.

With these linkages and assumptions, we construct aggregate data of actual site choices for each CBG from 2018 to 2021. Our final estimation data set consists of 2,840,714 observations corresponding to CBG/site/year combinations where sampling occurred from 2018 to 2021. These observations are constructed from individual cell phone devices in 216,073 CBGs across the nation. These residents took a total of 1,364 million trips, or 6,312 trips per CBG over our study period. On average, recreators traveled 57 miles and took 1.2 hours for a one-way-trip visit. The average travel costs are about $80 between 2018 and 2021. Table 1 provides more details about our final sample[23].

Table A1 shows the annual recreation visits in Safegraph sample from 2018 to 2021, averaged over site type and year[24]. To make it comparable over time, we consider 2018 as the base year and use the ratio of the total number of devices at any given year to the total number of devices in 2018 as weights to adjust the average annual recreation visits for each site type. We obtained 32,145 unique destinations from the SafeGraph data, out of which 21,131 (65.7%) are parks, 1,206 (3.8%) are river and lake sites, and 2,101 (6.5%) are open space. This table shows an expected pattern within each type, with annual visits lowest in 2018 and peaking in 2019. As the pandemic hits the U.S., many recreation sites were closed temporally and the number of trips to all sites went down except for lake recreation sites. When it comes to 2021, restrictions have become relaxed or lifted and the visits bounce back to a higher level.

Figure 1 shows how these sites are distributed across the nation. In general, people are less likely to have access to these recreational resources in the Midwest region than those living in the coastal area. Park

[22]We also consider alternative market sizes to test the robustness of our results. For example, For people from CBGs adjacent to the university, they are more likely to be students and have more free time to visit recreation sites. We consider 190 days (including additional summer time) and 365 days (full year) as the alternative market sizes.

[23]It is worth noting that, in our data, recreation sites with water quality measures tend to have larger sizes. See more details in Appendix Table A2

[24]Site type is defined based on the location name of the recreation site. All types of sites included in Table A1 are identified as water-based recreation sites.

sites can be accessed almost everywhere, while Beach and Harbor sites are more likely to be located on the East and West coast, and Great Lakes region. Figure 2 presents how the recreation visits and Secchi depth evolved at each site during our study period. Before the pandemic, some sites had fewer visitors and some sites had more visitors. As the stay-at-home orders took effect across states, a significant number of recreation sites in the South region experienced a decline in visitation, while recreation sites in the Great Lakes and Northeast region had more visitors. As restrictions have become relaxed or lifted, travel and vacations have become more rampant, and recreation sites are seeing an uptick in tourists again. In terms of water quality, we do not find any clear pattern for Secchi depth measures over time. Figure 3 shows the spatial variation of visit changes and water quality changes, and their correlation. We find a great variation in visits while a relatively small variation in Secchi depth. The correlation plots suggest a positive relationship between the changes in recreation visits and changes in water quality.

3 MODEL

In this section, we specify a model of recreator behavior in order to estimate the recreation welfare effects of water quality changes. We use a discrete-choice model following the framework of Berry et al. (1995). Each period, recreators make a decision to visit one of the recreation sites in their choice sets, or the outside good, any other activities that are not defined as water-based recreation activities. The demand model is static in that recreators choose myopically, without taking into account the future evolution of travel costs and other site characteristics.

More specifically, the utility function of visitor i to recreational site j in market t is as follows:

$$U_{ijt} = \delta_{ijt} + \mu_{ijt} + \epsilon_{ijt}, \tag{2}$$

where δ_{ijt} represents the mean utility of site j for visitor from CBG i, and μ_{ijt} denotes the individual-specific preference deviation from the mean utility. ϵ_{ijt} follows i.i.d. Type-I extreme value distribution. The mean utility δ_{ijt} is defined as:

$$\delta_{ijt} = \alpha TC_{ijt} + \beta_1 WQ_{jt} + \beta_2 \text{COVID}_t + \beta_3 WQ_{jt} \times \text{COVID}_t + \beta_4 W_{jt} + \beta_5 X_{jt} + \gamma_i + \zeta_j + \xi_{jt}, \tag{3}$$

where TC_{ijt} denotes the travel costs from the centroid of census block group i to site j at market t; WQ_{jt} denotes the water quality measures at site j and year t. We include a COVID dummy, a state-year level lockdown dummy, and county-year level log of cumulative COVID cases to control for the pandemic impacts and allow for the demand curve to shift. We interact the COVID dummy with water quality measures to permit preference changes in terms of water quality. W_{jt} denotes the weather condition at site

j and year t. We characterize temperature and precipitation using a binning approach. In particular, we create sets of dummies where average temperature and precipitation fell into one of 10 decile bins. We include site fixed effects ζ_j to capture time-invariant unobserved site attributes and CBG fixed effects to capture unobserved demographic variables that influence the demand for outdoor recreation. Finally,

The individual deviation from the mean utility is defined as

$$\mu_{ijt} = \sigma_{tc} TC_{ijt} \nu_{i,tc} + \sigma_{wq} WQ_{jt} \nu_{i,wq} + \sigma_c \text{COVID}_t + \sigma_{wqc} WQ_{jt} \times \text{COVID}_t \nu_{i,wqc} \tag{4}$$

where $\nu_{i,tc}$, $\nu_{i,wq}$, $\nu_{i,c}$ and $\nu_{i,wqc}$ are standard normal draws. Each visitor i makes a discrete choice and chooses the site j at market t that maximizes her/his random utility U_{ijt}. The discrete choice model allows opting out. Thus, an "outside good" is introduced into the model. The outside good in our case is all other activities that do not qualify as recreation. The mean utility of the outside good is normalized to $U_{i0} = \epsilon_{i0}$.

Assuming that the random utility terms follow the extreme value distributional assumption, the probability that a utility-maximizing visitor i will choose attraction j = 1 … J in market t takes the following form:

$$share_{jt} = \int \frac{exp(\delta_{jt} + \mu_{ijt})}{\sum_k exp(\delta_{kt} + \mu_{ikt})} d\nu_i \tag{5}$$

We leverage panel data and include site fixed effects to control for spatial unobserved factors. There is the possibility that travel costs are correlated with time-varying unobserved site-specific utility ξ_{jt} through changes in local demand for gasoline or increases in travel time through congestion. Therefore, instruments are needed to identify the parameter for travel costs. We argue that the interactions between average crude oil prices and state dummies are uncorrelated with demand shocks ξ_{jt}, which control for national factors that do not vary across markets, such as national fuel price shocks. We also argue the travel distance from the origin i to recreation site j is uncorrelated with demand shocks ξ_{jt} as these are given in the short run for each visitor. The identifying assumption is that for a vector of instruments Z_{tc},

$$E[Z_{tc} \xi(\theta_2)] = 0 \tag{6}$$

The following equation sets the basis for the estimation of the demand model. We estimate the market share system with a general method of moments estimator. For every parameter guess, we invert the market system using a contraction mapping to obtain $\xi(\theta_2)$. Define Z_{tc} to be the matrix of instruments and A_{tc} a weighting matrix. We estimate θ_2 by:

$$\min \quad \xi(\theta_2)' Z_{tc} A_{tc} Z_{tc}' \xi(\theta_2) \tag{7}$$

4 RESULTS

Table 2 shows results from a logit model, where we assume no visitor taste heterogeneity on travel distance and water quality, using Secchi depth as the measure of water quality. In other words, $\sigma = 0$.[25] We start with a model that includes CBG and county fixed effects (column 1), a second model with CBG and site fixed effects (column 2), a third model with additional weather controls (column 3), a fourth model with weather and pandemic controls, and a fifth model with a flexible preference on water quality (column 5). Across specifications, the sign on the travel costs is negative, indicating that visitors are less likely to visit a site if they need to travel a longer distance in a trip. Our preferred specification (column 6) uses the interaction between crude oil prices and state dummies, and travel distance as instruments for travel costs to address potential endogeneity issues discussed above. The instruments are strong, with a Kleibergen-Paap F score of 2125. Using these instruments slightly increase the magnitude of the travel cost coefficients from -0.0036 to -0.0039, suggesting there is little to no correlation between travel costs and time-varying unobservable attributes in our sample.

We are particularly interested in the marginal utility of our water quality measure, represented by the average annual Secchi depth at each site. Comparing the results from column 1 to column 3, we show the importance of including the site fixed effects and weather conditions to control for the impact of the spatial unobserved factors as well as the weather on recreation demand. In column 4, as we include the COVID dummy, the magnitude of Secchi depth coefficients decreases from 0.029 to 0.010, suggesting that the pandemic not only influences the demand for outdoor recreation but also affects the water quality as well. In column 5, we allow for preference changes in water quality before and during the COVID. The coefficient of Secchi depth gives the baseline estimated marginal utility of Secchi depth for people living in a CBG having the sample average median household income in the pre-COVID period. The coefficient of the interaction term gives the changes in the marginal utility of Secchi depth during the pandemic relative to the pre-COVID period. We find evidence of no preference change in water quality in both column 5 and column 6. To put it in monetary value, we calculate the marginal willingness to pay for Secchi depth by dividing the water quality coefficient by the negative value of the travel cost coefficient. We find that, for an average recreator, the willingness to pay for a 1-meter increase in Secchi depth has a 95% confidence interval ranging from $2.52 to $2.59, with a mean of $2.55, which is in line with previous recreation demand studies (Ji et al. (2020)) where they find the marginal willingness to pay is about $5-$10 per household.

We also explore the spatial heterogeneity of water quality impact across census regions. Table 3 reports the

[25] We follow Berry (1994) and use linear regression to produce these estimates.

recreation demand estimates by census regions. We observe similar positive marginal utility of Secchi depth in the pre-COVID period with slight differences in magnitude across regions. However, the preference for water quality shifted in different directions during the pandemic. For example, recreators in the Northeast, South, and West regions gained a higher marginal utility of water quality during the pandemic, while Midwest recreators had a lower marginal utility gain from water quality improvements. Across the different regions of our analysis, recreators in the Northeast region are willing to pay an average of $2.16 for marginal change in Secchi depth, while people in the South region are only willing to pay $1.31 for the changes. These differences could be due to data limitations as the total observation of non-West regions only accounts for less than half of the sample in our analysis.

We conduct a number of robustness checks. First, we run our preferred model with alternative polygon buffers and report the results in Appendix Table C1. We consider adjusted site polygons with 100m, 200m, 300m, 400m, and 500m buffers. The coefficients are relatively similar across the model variants except for the 100m buffer. This could be due to the fact that a 100m buffer is not large enough to cover the water bodies that recreators observed. Second, we run our preferred model with alternative travel cost definitions, including actual travel costs, travel costs excluding the value of travel time, and travel costs including the full value of travel time (Appendix Table C2). In general, these results show slightly different impacts on recreational visits and the coefficients of travel costs vary due to the definition changes, which suggests that the value of travel time plays an important role in understanding recreational behavior.

One concern about our sample is whether we include most of the single-day car-trip visits. Here, we re-estimate our model with alternative car-mode trip cutoffs, including a 200-mile, 250-mile, 350-mile, and 400-mile cutoff (Appendix Table C3). We find the coefficient of Secchi depth decreases as the cutoff increases, while the changes become negligible when the cutoff is larger than 300 miles. In addition to that, the marginal willingness to pay is robust across all specifications. We also explore the alternative function form such as water quality dummies or log form of water quality (Appendix Table C4). Results show significant effects of water quality on recreation visits for Secchi depth and Chlorophyll-a across different function forms.

Recreators might expect to encounter many other recreators during a visit to a popular site based on prior experience on this particular site. Some degree of congestion may be desirable as there are pleasant social interactions among like-minded participants at most destinations. However, this might not be the case during the pandemic, when people might think a popular site is "too crowded". Here, we use a set of

congestion variables, such as visits, visitors, and relative visits/visitors at a site, and a quadratic form of these variables to test the robustness of our results. The relative visits/visitors are defined as the share of visits or visitors to a site to the total visits from a CBG in a year[26]. To capture the prior experience with congestion, all the congestion variables use the previous year's data. We present our results in Appendix Table C5. The coefficients of Secchi depth are slightly larger than the one in our base model and the marginal willingness to pay varies between \$2.5 and \$3.5 across all specifications. This suggests the robustness of our results even after controlling for the impact of prior congestion experience.

Another assumption we make about the "recreation market" is that the total market size of a CBG is the multiplication of the average annual number of the device at a CBG and the number of holidays and weekends over a year (115 days), which might not be true for students and other part-time employees. Therefore, we consider several potential market sizes, including the number of holidays, weekends, and summer/winter vacations over a year (190 days), a full year(365 days), 115 days for general CBGs and 190 days for CBGs adjacent to the university, and 115 days for general CBGs and 365 days for CBGs adjacent to the university. We report our results in Appendix Table C6. Our results are robust across specifications.

Finally, we consider alternative cutoffs for the lower bound of site size and annual visits, including no restriction on size and visits, sites above 1 Hectare, sites above 2 Hectares, and sites above 2 Hectare and annual visits more than 1,000. We report results in Appendix Table C7. We find the coefficients of Secchi depth decrease slightly when we restrict our sample to sites the size is above 2 Hectares. We also find similar results that little to no preference changes for water quality during the pandemic using alternative cutoffs. Overall, the results are pretty robust across all specifications.

5 THE VALUE OF WATER QUALITY IN RECREATION SITES

In this section, we consider Secchi depth as our main water quality measure and quantify the welfare effects of three water quality scenarios using our estimated model of recreation demand. We first assess the recreation benefits from water quality improvements by simulating the compensating variation for all the recreation sites experiencing improvements in water quality to the level of cleanest site[27]. Throughout the counterfactual analysis, we assume that recreation sites do not change other attributes due to the changes in water quality. We also assume that visitors spent the same travel costs visiting sites in their choice

[26] A measure of relative congestion, consisting of visits to a given site as a share of all visits to all sites, has been used previously in the literature (Kolstoe and Cameron (2017); Murdock (2006); Phaneuf et al. (2009); Timmins and Murdock (2007)).

[27] We define the cleanest lake as the lakes with highest average Secchi Depth measures over our study period. To avoid the extreme outlier driving the results, we use the 99 percentile of the water quality distribution (9 meters) in the cleanest site as our counterfactual measures.

sets. Given the richness of our data, we are able to use recreation preferences for water quality before the pandemic and investigate the welfare effects of non-marginal changes in water quality when the restrictions on recreation sites were relaxed in 2021. Assuming no taste heterogeneity on water quality and travel costs, the utility function we use for the counterfactual analysis is:

$$V_{ijt}^{new} = \hat{\alpha} TC_{ijt} + \hat{\beta}_1 WQ_{jt} + \hat{\beta}_4 W_{jt} + \gamma_i + \zeta_j + \epsilon_{ijt} \tag{6}$$

The baseline scenario uses the real water quality measures in 2021, and the predicted water quality change scenario is constructed by improving the water quality of all sites to the 99 percentile of Secchi depth distribution in the cleanest lake in 2021. The non-marginal water quality improvements use the basic compensating variation formula:

$$CV_i^{Cleanest} = -\frac{1}{\alpha}(log(\sum_{j=0}^{J} exp(V_{ij}^{new}|q_1)) - log(\sum_{j=0}^{J} exp(V_{ij}^{new}|q_0))) \tag{7}$$

CV_i is then estimated by calculating the expected changes in utility resulting from non-marginal changes in water quality. We also rerun our preferred model using data from each census region to explore the spatial heterogeneity of these welfare changes.

Next, we calculate the welfare changes under two site closure scenarios that are most likely to be considered by local authorities over our study period: 1) closing the most polluted recreation sites (Secchi depth < 0.5 meters); 2) closing the most popular recreation destinations. Similarly, we rerun the regression within each census region under each scenario. Without loss of generality, we assume it is site 1, the compensating variation associated with the closure of a single site is as follows:

$$CV_i^{Closure} = -\frac{1}{\alpha}(log(\sum_{j=0}^{J'} exp(V_{ij}^{new}|q_0)) - log(\sum_{j=0}^{J} exp(V_{ij}^{new}|q_0))) \tag{8}$$

Table 4 shows the counterfactual changes under each water quality scenario. Row 1 of Table 4 explores how the welfare changes for non-marginal changes in Secchi depth in 2021, Our preferred model predicts an average of \$18.36 welfare per capita gains for recreation visitors if the Secchi depth of all sites were improved to 9 meters nationwide in 2021. The spatial heterogeneity is shown in columns 2-4 of Table 4. we find that the mean monetary compensation per capita is highest for visitors in the Northeast region at \$16.31 and lowest at \$9.92 for visitors in the South region. A simple back-of-the-envelope calculation of welfare impacts would be to multiply the welfare gains from water quality changes by the sample considered in our study. We find that annual welfare gains would be \$433.26 million when the water quality was improved at all the recreation sites to the 99 percentile of Secchi depth distribution in the cleanest site. Across the

different regions of our analysis, the Northeast region experiences annual gains of about $60.13 million and the Midwest region experiences annual gains of about $74.07 million.

Table 4 also reports the welfare changes when closing the most polluted and most popular sites. We find an average of $37.22 and $115.32 annual welfare loss per capita due to the closures of the most polluted sites and most popular sites. Looking closer at regional heterogeneity, we find that the mean monetary compensation per capita to close the most popular site is highest for visitors in the Northeast region at $132.36 and lowest at $98.75 for visitors in the West region. In contrast, we find that the mean monetary compensation per capita to close the most polluted site is highest for visitors in the Northeast region at $48.83 and lowest at $16.26 for visitors in the West region. A simple back-of-the-envelope calculation suggests that annual welfare losses would be $2.7 billion and $878.37 million under these two site closure scenarios. Across the different regions of our analysis, the census regions experience annual losses ranging from $445.34 million to $1 billion for closing the most popular sites and $73.33 million to $464.54 million for closing the most polluted sites, respectively.

6 DISCUSSION

Our study shows that water quality is likely a strong driver of recreation behavior and welfare changes from 2018 to 2021. Using the random coefficient logit model, we have found that the welfare gain due to the improvements in water quality is in order of almost half a billion US dollars. Furthermore, the welfare losses due to closing the most popular sites and the most polluted sites for each CBG could be substantial. However, these estimates are conservative in many ways. First, our welfare analysis does not consider the general equilibrium changes due to the non-marginal changes in water quality. Second, it does not reflect "nonuse" or "existence" values for clean water due to its pure existence and divorced from any specific uses. Finally, our estimates ignore potential health benefits generated from the improvements in water quality in recreation sites.

The compensating variation estimated in our paper is inversely proportional to the recreators' response to travel costs and directly proportional to their response to water quality in recreation sites. For instance, the response of visitors in the West region to travel costs is the largest of the four census regions, showing that visitors in the West region are less willing to travel long distances than visitors in other places. A possible explanation is that visitors in the West region have less access to recreation sites than visitors in other regions. Since the compensation measure is inversely related to the response to travel costs, this makes the compensation measure for visitors in the West region slightly smaller than that in the Northeast

and Midwest regions. Our results also suggest that visitors exhibit heterogeneous preferences for water quality in different regions.

Direct comparison of our results to those of previous water quality studies is imperfect due to the national scope of our study. Vesterinen et al. (2010) utilizes national recreation inventory data combined with water quality data to model recreation participation and estimate the benefits of water quality improvements in Finland. A water policy scenario with a 1-m improvement in water clarity for both inland and coastal waters from their study indicates that the consumer surplus would increase $10-$30 per swimmer and $20-$60 per fisher. Czajkowski et al. (2020) estimates a spatially explicit travel cost model of coastal site recreation to the Baltic Sea to assess the welfare of accessing individual sites. Their results suggest improving water quality to blue flag status, where Secchi depth is less than 1 meter, boosts the recreational value by 47-247 EUR per trip. More recently, Merrill et al. (2022) utilizes water quality metrics derived from remotely sensed images and uses a travel cost model framework to estimate the value of water quality for coastal recreation in New England. They find a $4-$5 change for a meter in clarity and the welfare gains from a 20% increase in Secchi depth is $0.07 per person per trip. This leads to an aggregate annual benefit of $5.7 million for a 20% increase in Secchi depth in Cap Code. Compared to these studies, our measure of compensable gains is slightly smaller. One potential reason is that these studies focus on the gains from large recreation sites, while our study includes many large state parks but also those small recreation sites.

How do these compensating estimates compare to the costs incurred to achieve the water quality gains since the 1972 Clean Water Act? Over the period 1970 to 2014, The United States has spent $2.83 trillion to clean up surface water pollution, $1.99 trillion to provide clean drinking water, and $2.11 trillion to clean up air pollution ($2017 dollars)(Keiser and Shapiro (2019b)). For surface water regulations, 67 percent of regulations fail a benefit-cost test with a 0.79 benefit-cost ratio from 1992 to 2017. Based on the recent annual spending on surface water pollution and population estimates, an average American needs to pay for $227 for clean surface water but only gains $179 from the water quality improvements. Keiser and Shapiro (2019a) examines how CWA grants the federal government gave to cities to improve wastewater treatment affected US surface water quality. Through these grants, they find the Total Suspended Solids decreased by 26.36 mg/L from 1972 to 2021 relative to the pre-1972 period. We convert the percentage changes in TSS to percentage changes in Secchi depth, using the calibrated parameters from Baughman et al. (2015) and Al-Yaseri et al. (2013). A 52.98% decrease (26.36/49.75) in TSS is equivalent to an 84.66% increase in Secchi depth. We then calculate the compensating variation where the counterfactual scenario is constructed by improving the water quality of all sites by 84.66% in 2021. The results suggest an average of

$3.08 welfare per capita gains for recreation visitors if counterfactual happened. If we consider these benefit estimates are additive to the current benefits number, our findings add 1.7% to the previously estimated benefits gained from the Clean Water Act.

The available data on surface water pollution is still poor. Compared to ambient pollution, measuring water pollution is less common and standardized; water pollution emissions are often self-reported and systematically suffer from nonreporting; data on health outcomes for water-based recreation are way more limited. Besides that, since many organizations collect water pollution data, using a range of methods and devices, it can be even more complex to determine which water quality data are accurate, representative, and comparable. In recent years, a growing literature has been mapping the water quality parameters using satellite images over inland lakes (Barrett and Frazier (2016); Chandrasekar et al. (2010); Liu et al. (2017); Molkov et al. (2019); Olmanson et al. (2008); Pahlevan et al. (2017); Potes et al. (2011, 2012, 2018); Toming et al. (2016)). Several empirical and structural methods have been explored to provide reliable estimates for the spatial and temporal cover of water quality parameters. Here, we apply the quasi-analytic algorithm by Lee et al. (2016) to data from the Sentinel-2 mission (Multi-Spectral Instrument (MSI)). By averaging the Secchi depth measures from each polygon, we validate the satellite estimates with in-situ water quality data from Water Quality Portal in Appendix Figure B4 and B5. Results show a strong correlation between the satellite estimates and in-situ data over years in our sample. More efforts could be undertaken in this area to help enrich the water quality database and have a better understanding of recreation behavior for all recreation sites.

7 CONCLUSION

This paper extends the literature on examining the effects of water quality on recreation demand using innovative cell phone data. By developing a random utility site choice model, we demonstrate the feasibility of using cell phone data to estimate the value of water quality in water-based recreation sites. Results from our preferred model suggest that water quality is likely a strong driver of recreation behavior changes over our study period. Recreators are willing to pay an average of $2.55 for a 1-meter increase in Secchi depth in the sites they visited. Furthermore, we find some evidence of spatial heterogeneity in water quality preference such that the MWTP for Secchi depth varies from $1.3 to $2.2 across census regions. We simulate three water quality scenarios that show a significant willingness to pay for water quality improvements and avoiding site closure. We find the benefits from improving the water quality of all sites to the level of the cleanest site is $433.26 million, with spatial heterogeneity across census regions ranging from $50.7 million to $ 100.4 million. Additionally, the welfare losses due to the most popular and polluted site closure

are $2.7 billion and $878.37 million, respectively. Revisiting the water quality changes from 1972 to 2001, Our findings add 1.7% to the previously estimated benefits gained from the Clean Water Act.

Our results are subject to a few important caveats. First, the cell phone data has several limitations on our analysis. Safegraph collects location information through cell phone GPS, the data could thus be under-representing elderly and low-income individuals. Even though evidence has been shown that the general visitation data is U.S. representative at the state and county level, it is not clear whether the recreation visit samples are representative at any geography level. Given that, we suggest caution in interpreting our welfare results for the general population. Second, our logit model helps us quantify the effects of water quality on recreation demand but relies on the assumption that recreators leave the market after visiting recreation sites and do not visit again at each period. Third, our results are limited by assuming visitors participated in similar activities to the recreation sites. Water bodies provide a series of water-related services to humans, such as boating, swimming, or fishing. Failing to link the recreation activities to visitation significantly limited our analysis to understand the value of water quality across different water-related services. Our welfare estimates in the first scenario should be interpreted as the average value of water quality improvements across all types of recreation activities. Last, we are also limited by the availability of water quality data. Despite the great efforts we have devoted to collecting and imputing the water quality data, the data limitation precludes us explore recreation behavior across all the water-based recreation sites. Our welfare estimates assume recreators have similar responses to water quality changes in recreation sites where water quality measures are not available.

Despite these limitations, our modeling approach provides a starting point for providing national estimates of the overall impacts of water quality on outdoor recreation. The framework of this paper can be applied to study other settings such as estimating the effectiveness of early warning systems for harmful algal blooms or evaluating the water quality monitoring and mitigation programs. Our paper motivates two lines of future work. First, The new innovative data such as cell phone records and social media geotagged data provide a new solution to gather environmental data at high temporal frequency and spatial resolution. More calibration and external validity checks are needed to understand the plausibility of the data on recreation demand studies. Second, a growing remote sensing literature leverages the information from satellite images to calibrate the satellite estimates of inland water quality. More efforts could be undertaken in this area to help enrich the water quality database and facilitate the development of models for environmental research.

REFERENCES

Al-Yaseri, I., S. Morgan, and W. Retzlaff (2013). Using turbidity to determine total suspended solids in storm-water runoff from green roofs. *Journal of Environmental Engineering 139*(6), 822–828.

Barrett, D. C. and A. E. Frazier (2016). Automated method for monitoring water quality using landsat imagery. *Water 8*(6), 257.

Baughman, C. A., B. M. Jones, K. K. Bartz, D. B. Young, and C. E. Zimmerman (2015). Reconstructing turbidity in a glacially influenced lake using the landsat tm and etm+ surface reflectance climate data record archive, lake clark, alaska. *Remote Sensing 7*(10), 13692–13710.

Berry, S., J. Levinsohn, and A. Pakes (1995). Automobile prices in market equilibrium. *Econometrica: Journal of the Econometric Society*, 841–890.

Berry, S. T. (1994). Estimating discrete-choice models of product differentiation. *The RAND Journal of Economics*, 242–262.

Chandrasekar, K., M. Sesha Sai, P. Roy, and R. Dwevedi (2010). Land surface water index (lswi) response to rainfall and ndvi using the modis vegetation index product. *International Journal of Remote Sensing 31*(15), 3987–4005.

Connelly, N. and T. Brown (2011). Effect of recall period on annual freshwater fishing effort estimates in new york. *Fisheries Management and Ecology 18*(1), 83–87.

Czajkowski, M., M. Zandersen, U. Aslam, I. Angelidis, T. Becker, W. Budziński, K. Zagórska, et al. (2020). Recreational value of the baltic sea: a spatially explicit site choice model accounting for environmental conditions. Technical report, Working papers 2018-11, Faculty of Economic Sciences, University of Warsaw ....

Dillman, D. A. (2017). *The promise and challenge of pushing respondents to the web in mixed-mode surveys*. Statistics Canada.

Dundas, S. J. and R. H. von Haefen (2020). The effects of weather on recreational fishing demand and adaptation: implications for a changing climate. *Journal of the Association of Environmental and Resource Economists 7*(2), 209–242.

Egan, K. J., J. A. Herriges, C. L. Kling, and J. A. Downing (2009). Valuing water quality as a function of water quality measures. *American Journal of Agricultural Economics 91*(1), 106–123.

Fenichel, E. P., J. K. Abbott, and B. Huang (2013). Modelling angler behaviour as a part of the management system: synthesizing a multi-disciplinary literature. *Fish and fisheries 14*(2), 137–157.

Ghermandi, A. (2018). Integrating social media analysis and revealed preference methods to value the recreation services of ecologically engineered wetlands. *Ecosystem services 31*, 351–357.

Hushak, L. J., J. M. Winslow, and N. Dutta (1988). Economic value of great lakes sportfishing: The case of private-boat fishing in ohios lake erie. *Transactions of the American Fisheries Society 117*(4), 363–373.

Hynes, S., D. Tinch, and N. Hanley (2013). Valuing improvements to coastal waters using choice experiments: An application to revisions of the eu bathing waters directive. *Marine Policy 40*, 137–144.

Ji, Y., D. A. Keiser, and C. L. Kling (2020). Temporal reliability of welfare estimates from revealed preferences. *Journal of the Association of Environmental and Resource Economists 7*(4), 659–686.

Keeler, B. L., S. A. Wood, S. Polasky, C. Kling, C. T. Filstrup, and J. A. Downing (2015). Recreational demand for clean water: evidence from geotagged photographs by visitors to lakes. *Frontiers in Ecology and the Environment 13*(2), 76–81.

Keiser, D. A. and J. S. Shapiro (2019a). Consequences of the clean water act and the demand for water quality. *The Quarterly Journal of Economics 134*(1), 349–396.

Keiser, D. A. and J. S. Shapiro (2019b). Us water pollution regulation over the past half century: burning waters to crystal springs? *Journal of Economic Perspectives 33*(4), 51–75.

Kelch, D., F. Lichtkoppler, B. Sohngen, and A. Daigneault (2006). The value of steelhead (onchorhynchus mykiss) angling in lake erie tributaries. *Journal of Great Lakes Research 32*(3), 424–433.

Kolstoe, S. and T. A. Cameron (2017). The non-market value of birding sites and the marginal value of additional species: biodiversity in a random utility model of site choice by ebird members. *Ecological economics 137*, 1–12.

Kubo, T., S. Uryu, H. Yamano, T. Tsuge, T. Yamakita, and Y. Shirayama (2020). Mobile phone network data reveal nationwide economic value of coastal tourism under climate change. *Tourism Management 77*, 104010.

Lee, Z., S. Shang, L. Qi, J. Yan, and G. Lin (2016). A semi-analytical scheme to estimate secchi-disk depth from landsat-8 measurements. *Remote sensing of environment 177*, 101–106.

Liu, H., Q. Li, T. Shi, S. Hu, G. Wu, and Q. Zhou (2017). Application of sentinel 2 msi images to retrieve suspended particulate matter concentrations in poyang lake. *Remote Sensing 9*(7), 761.

Loomis, J., B. Roach, F. Ward, and R. Ready (1995). Testing transferability of recreation demand models across regions: a study of corps of engineer reservoirs. *Water Resources Research 31*(3), 721–730.

Lupi, F., J. P. Hoehn, and G. C. Christie (2003). Using an economic model of recreational fishing to evaluate the benefits of sea lamprey (petromyzon marinus) control on the st. marys river. *Journal of Great Lakes Research 29*, 742–754.

Lupi, F., D. J. Phaneuf, and R. H. von Haefen (2020). Best practices for implementing recreation demand models. *Review of Environmental Economics and Policy*.

Melstrom, R. T. and F. Lupi (2013). Valuing recreational fishing in the great lakes. *North American Journal of Fisheries Management 33*(6), 1184–1193.

Merrill, N., M. Mazzotta, K. Mulvaney, J. Sawyer, J. Twichell, S. Atkinson, D. Keith, and L. Erban (2022). The value of water quality for coastal recreation in new england, usa.

Merrill, N. H., S. F. Atkinson, K. K. Mulvaney, M. J. Mazzotta, and J. Bousquin (2020). Using data derived from cellular phone locations to estimate visitation to natural areas: An application to water recreation in new england, usa. *PloS one 15*(4), e0231863.

Moeltner, K. and J. Englin (2004). Choice behavior under time-variant quality: State dependence versus "play-it-by-ear" in selecting ski resorts. *Journal of Business & Economic Statistics 22*(2), 214–224.

Molkov, A. A., S. V. Fedorov, V. V. Pelevin, and E. N. Korchemkina (2019). Regional models for high-resolution retrieval of chlorophyll a and tsm concentrations in the gorky reservoir by sentinel-2 imagery. *Remote Sensing 11*(10), 1215.

Morey, E. R., R. D. Rowe, and M. Watson (1993). A repeated nested-logit model of atlantic salmon fishing. *American Journal of Agricultural Economics 75*(3), 578–592.

Murdock, J. (2006). Handling unobserved site characteristics in random utility models of recreation demand. *Journal of environmental economics and management 51*(1), 1–25.

Nevo, A. (2001). Measuring market power in the ready-to-eat cereal industry. *Econometrica 69*(2), 307–342.

Newbold, S. C., S. Lindley, S. Albeke, J. Viers, G. Parsons, and R. Johnston (2022). Valuing satellite data for harmful algal bloom early warning systems.

Olmanson, L. G., M. E. Bauer, and P. L. Brezonik (2008). A 20-year landsat water clarity census of minnesota's 10,000 lakes. *Remote Sensing of Environment 112*(11), 4086–4097.

Pahlevan, N., S. Sarkar, B. Franz, S. Balasubramanian, and J. He (2017). Sentinel-2 multispectral instrument (msi) data processing for aquatic science applications: Demonstrations and validations. *Remote sensing of environment 201*, 47–56.

Palmquist, R. B., D. J. Phaneuf, and V. K. Smith (2010). Short run constraints and the increasing marginal value of time in recreation. *Environmental and Resource Economics 46*(1), 19–41.

Parsons, G., C. G. Leggett, J. Herriges, K. Boyle, N. Bockstael, and Z. Chen (2021). A site-portfolio model for multiple-destination recreation trips: Valuing trips to national parks in the southwestern united states. *Journal of the Association of Environmental and Resource Economists 8*(1), 1–25.

Parsons, G. R. and A. B. Hauber (1998). Spatial boundaries and choice set definition in a random utility model of recreation demand. *Land economics*, 32–48.

Parsons, G. R., A. J. Plantinga, and K. J. Boyle (2000). Narrow choice sets in a random utility model of recreation demand. *Land Economics*, 86–99.

Phaneuf, D. J., J. C. Carbone, and J. A. Herriges (2009). Non-price equilibria for non-marketed goods. *Journal of Environmental Economics and Management 57*(1), 45–64.

Phaneuf, D. J., C. L. Kling, and J. A. Herriges (2000). Estimation and welfare calculations in a generalized corner solution model with an application to recreation demand. *Review of Economics and Statistics 82*(1), 83–92.

Phaneuf, D. J. and V. K. Smith (2005). Recreation demand models. *Handbook of environmental economics 2*, 671–761.

Potes, M., M. J. Costa, J. Da Silva, A. M. Silva, and M. Morais (2011). Remote sensing of water quality parameters over alqueva reservoir in the south of portugal. *International Journal of Remote Sensing 32*(12), 3373–3388.

Potes, M., M. J. Costa, and R. Salgado (2012). Satellite remote sensing of water turbidity in alqueva reservoir and implications on lake modelling. *Hydrology and Earth System Sciences 16*(6), 1623–1633.

Potes, M., G. Rodrigues, A. M. Penha, M. H. Novais, M. J. Costa, R. Salgado, and M. M. Morais (2018). Use of sentinel 2–msi for water quality monitoring at alqueva reservoir, portugal. *Proceedings of IAHS 380*, 73–79.

Provencher, B. and R. C. Bishop (1997). An estimable dynamic model of recreation behavior with an application to great lakes angling. *Journal of Environmental Economics and Management 33*(2), 107–127.

Rolfe, J., R. J. Johnston, R. S. Rosenberger, and R. Brouwer (2015). Introduction: Benefit transfer of environmental and resource values. In *Benefit transfer of environmental and resource values*, pp. 3–17. Springer.

Rosenberger, R. S. and J. B. Loomis (2017). Benefit transfer. In *A primer on nonmarket valuation*, pp. 431–462. Springer.

Ross, M. R., S. N. Topp, A. P. Appling, X. Yang, C. Kuhn, D. Butman, M. Simard, and T. M. Pavelsky (2019). Aquasat: A data set to enable remote sensing of water quality for inland waters. *Water Resources Research 55*(11), 10012–10025.

Rubin, D. B. (1976). Inference and missing data. *Biometrika 63*(3), 581–592.

Rylander, R. G., D. B. Propst, and T. R. McMurtry (1995). Nonresponse and recall biases in a survey of traveler spending. *Journal of Travel Research 33*(4), 39–45.

Sinclair, M., A. Ghermandi, and A. M. Sheela (2018). A crowdsourced valuation of recreational ecosystem

services using social media data: An application to a tropical wetland in india. *Science of the Total Environment 642*, 356–365.

Sonter, L. J., K. B. Watson, S. A. Wood, and T. H. Ricketts (2016). Spatial and temporal dynamics and value of nature-based recreation, estimated via social media. *PLoS one 11*(9), e0162372.

Spalding, M., L. Burke, S. A. Wood, J. Ashpole, J. Hutchison, and P. Zu Ermgassen (2017). Mapping the global value and distribution of coral reef tourism. *Marine Policy 82*, 104–113.

Tarrant, M. A., M. J. Manfredo, P. B. Bayley, and R. Hess (1993). Effects of recall bias and nonresponse bias on self-report estimates of angling participation. *North American Journal of Fisheries Management 13*(2), 217–222.

Timmins, C. and J. Murdock (2007). A revealed preference approach to the measurement of congestion in travel cost models. *Journal of Environmental Economics and management 53*(2), 230–249.

Toming, K., T. Kutser, A. Laas, M. Sepp, B. Paavel, and T. Nõges (2016). First experiences in mapping lake water quality parameters with sentinel-2 msi imagery. *Remote Sensing 8*(8), 640.

Van Houtven, G., C. Mansfield, D. J. Phaneuf, R. von Haefen, B. Milstead, M. A. Kenney, and K. H. Reckhow (2014). Combining expert elicitation and stated preference methods to value ecosystem services from improved lake water quality. *Ecological Economics 99*, 40–52.

Vesterinen, J., E. Pouta, A. Huhtala, and M. Neuvonen (2010). Impacts of changes in water quality on recreation behavior and benefits in finland. *Journal of Environmental Management 91*(4), 984–994.

Viscusi, W. K., J. Huber, and J. Bell (2008). The economic value of water quality. *Environmental and Resource Economics 41*(2), 169–187.

Von Haefen, R. H. and D. J. Phaneuf (2003). Estimating preferences for outdoor recreation:: a comparison of continuous and count data demand system frameworks. *Journal of Environmental Economics and Management 45*(3), 612–630.

White, E. M., S. G. Winder, and S. A. Wood (2022). Applying novel visitation models using diverse social media to understand recreation change after wildfire and site closure. *Society & Natural Resources*, 1–18.

Whitehead, J. C., D. J. Phaneuf, C. F. Dumas, J. Herstine, J. Hill, and B. Buerger (2010). Convergent validity of revealed and stated recreation behavior with quality change: a comparison of multiple and single site demands. *Environmental and Resource Economics 45*(1), 91–112.

Wood, S. A., S. G. Winder, E. H. Lia, E. M. White, C. S. Crowley, and A. A. Milnor (2020). Next-generation visitation models using social media to estimate recreation on public lands. *Scientific reports 10*(1), 1–12.

Table 1. Summary Statistics

	Count	Mean	S.D.	Min	Max
Water Quality Measures					
Secchi Depth (m)	2,840,714	1.35	1.07	0.10	9.00
Secchi Depth > 1m	2,840,714	0.19	0.39	0.00	1.00
Dissolved Oxygen (mg/L)	5,286,139	7.78	1.78	0.06	14.30
Dissolved Oxygen> 8 mg/L	5,286,139	0.50	0.50	0.00	1.00
Travel Costs					
Travel Costs ($)	2,840,714	79.92	96.08	0.04	851.11
Regular Gas Prices ($)	2,840,714	11.11	1.67	7.81	17.88
Depreciation (cent)	2,840,714	22.90	1.81	21.43	26.00
Maintenance (cent)	2,840,714	8.96	0.47	8.21	9.55
Median Household Income ($1,000)	2,840,714	37.09	19.11	1.20	120.19
Travel Distance (mile)	2,840,714	56.61	69.58	0.01	300.00
Travel Duration (h)	2,840,714	1.21	1.35	0.00	8.70
Recreation Visits					
Visitors	2,840,714	14.12	78.40	4.00	44171.00
Outside Options	2,840,714	20549.77	32526.64	97.42	3,127,158
Trip Share	2,840,714	0.0010	0.0027	0.0000	0.2300
Outside Share	2,840,714	0.9530	0.0262	0.6003	0.9994
Area (Hectare)	2,840,714	32.52	103.66	1.00	6018.06
Dummy for University CBG	2,840,714	0.05	0.21	0.00	1.00
Weather Condition					
Mean Temparature (C)	2,840,714	16.21	5.82	2.14	26.89
Precipitation (mm)	2,840,714	1241.46	385.69	123.77	3226.29
Cumu. COVID cases	2,840,714	1,541,002	3,685,849	0.00	48,739,445
Cumu. COVID deaths	2,840,714	23953.53	58113.30	0.00	849402

Notes: Statistics for each variable are calculated only across the recreation sites with water quality measures. For travel costs, regular gas prices, maintenance, depreciation, and median household income variables, all means, standard deviations, minimums, and maximums are in CPI-deflated 2018 U.S. dollars. For additional details, see Section 2.

Table 2. Recreation Demand Regression Results

	(1) OLS	(2) OLS	(3) OLS	(4) OLS	(5) OLS	(6) IV
Travel Costs	-0.003***	-0.004***	-0.004***	-0.004***	-0.004***	-0.004***
	(0.000)	(0.000)	(0.000)	(0.000)	(0.000)	(0.000)
Secchi Depth	-0.006***	0.057***	0.029***	0.010***	0.010***	0.010***
	(0.001)	(0.002)	(0.002)	(0.002)	(0.002)	(0.002)
COVID				0.194***	0.194***	0.186***
				(0.010)	(0.010)	(0.002)
Secchi Depth X COVID					-0.000	-0.000
					(0.001)	(0.001)
ln(Cumu. Cases)				-0.002***	-0.002***	-0.002***
				(0.000)	(0.000)	(0.000)
Lockdown Dummy				0.022***	0.022***	0.022***
				(0.007)	(0.007)	(0.007)
Observations	2819946	2819946	2819946	2819946	2819946	2819946
N(BlockGroup)	155145	155145	155145	155145	155145	155145
CBG FEs	Yes	Yes	Yes	Yes	Yes	Yes
Site FEs		Yes	Yes	Yes	Yes	Yes
Weather FEs			Yes	Yes	Yes	Yes
MWTP	-1.949	15.116	7.618	2.512	2.551	2.554
Kleibergen-Paap F						2125

Notes: Table 2 shows the results of running the recreation demand model without visitor taste heterogeneity on travel distance and water quality. Column 1 includes county and CBG fixed effects; column 2 includes site and CBG fixed effects; column 3 adds additional weather controls; column 4 adds additional weather and pandemic controls; column 5 adds additional weather and pandemic controls, and interaction between Secchi depth and COVID dummy; column 6 uses the interaction between crude oil price and state dummies, and travel distances as instruments for travel costs (CPI-deflated to 2018 dollars). The standard error is clustered at CBG level. Robust standard errors are in parentheses. ***,**,* denotes statistical significance at the 1%, 5%, and 10% levels, respectively. For additional details, see Section 4.

Table 3. Spatial Heterogeneity: Recreation Demand Regression Results

	(1)US	(2)Northeast	(3)Midwest	(4)South	(5)West
Travel Costs	-0.004***	-0.004***	-0.004***	-0.004***	-0.007***
	(0.000)	(0.000)	(0.000)	(0.000)	(0.000)
Secchi Depth	0.010***	0.008	0.008***	0.005*	0.011**
	(0.002)	(0.005)	(0.003)	(0.003)	(0.005)
COVID	0.194***	0.457***	-0.987***	-1.348***	-1.152***
	(0.010)	(0.015)	(0.028)	(0.023)	(0.065)
Secchi Depth X COVID	-0.000	0.021***	-0.007***	0.014***	0.025***
	(0.001)	(0.002)	(0.001)	(0.002)	(0.002)
ln(Cumu. Cases)	-0.002***	-0.014***	0.063***	0.084***	0.067***
	(0.000)	(0.000)	(0.002)	(0.001)	(0.003)
Lockdown Dummy	0.022***	0.046***	-0.093***	-0.037**	0.050
	(0.007)	(0.013)	(0.011)	(0.016)	(0.048)
Observations	2819946	438040	678698	1511951	191215
N(BlockGroup)	155145	32572	39782	59829	22957
CBG FEs	Yes	Yes	Yes	Yes	Yes
Site FEs	Yes	Yes	Yes	Yes	Yes
Weather FEs	Yes	Yes	Yes	Yes	Yes
MWTP	2.551	2.162	1.972	1.315	1.723

Notes: Table 3 shows the spatial heterogeneity of running the recreation demand model without visitor taste heterogeneity on travel distance and water quality. Column 1 only includes recreation sites in the Northeast region; column 2 only includes recreation sites in the Midwest region; column 3 only includes recreation sites in the South region; column 4 only includes recreation sites in the West region. The standard error is clustered at CBG level. Robust standard errors are in parentheses. ***,**,* denotes statistical significance at the 1%, 5%, and 10% levels, respectively. For additional details, see Section 4.

Table 4. Annual Welfare Changes Under Water Quality Scenarios

	(1)US	(1)Northeast	(2)Midwest	(3)South	(4)West
Welfare Change per Capita ($)					
Scenario 1: Improve to	18.36	16.315	14.002	9.924	11.243
Cleanest Site Level	(17.85-18.86)	(14.76-17.86)	(13.22-14.78)	(9.18-10.66)	(10.41-12.07)
Scenario 2:WTP to Avoid	115.318	132.36	103.067	101.81	98.752
Most Popular Site Closure	(115.26-115.37)	(132.16-132.55)	(102.97-103.15)	(101.75-101.86)	(98.58-98.92)
Scenario 3: WTP to Avoid	37.222	48.833	20.769	45.937	16.26
Most Polluted Site Closure	(37.20-37.24)	(48.74-48.91)	(20.74-20.79)	(45.90-45.96)	(16.22-16.29)
Welfare Changes in Millions ($)					
Scenario 1: Improve to	433.263	60.128	74.072	100.36	50.701
Cleanest Site Level	(421.42-445.10)	(54.42-65.8)	(69.94-78.19)	(92.85-107.86)	(46.97-54.43)
Scenario 2:WTP to Avoid	2721.291	487.822	545.242	1029.565	445.341
Most Popular Site Closure	(2720.0-2722.5)	(487.10-488.53)	(544.77-545.70)	(1028.9-1030.1)	(444.58-446.1)
Scenario 3: WTP to Avoid	878.369	179.978	109.87	464.543	73.326
Most Polluted Site Closure	(877.89-878.84)	(179.66-180.29)	(109.75-109.98)	(464.25-464.83)	(73.16-73.48)

Notes: The estimate represents the mean welfare predictions under three water quality scenarios. For column (1), we run the recreation demand model without visitor taste heterogeneity on travel distance and water quality to produce the average estimate. For columns (2)-(4), we restrict the sample to each census region and produce the average estimate. Standard deviations of welfare estimates are in parentheses. For additional details, see Section 5. 95% confidence intervals for these medians are reported in parentheses based on the asymptotic distribution of the estimated demand coefficients. See more details in Nevo (2001).

Figure 1. National Map of Water-based Recreation Sites by Type

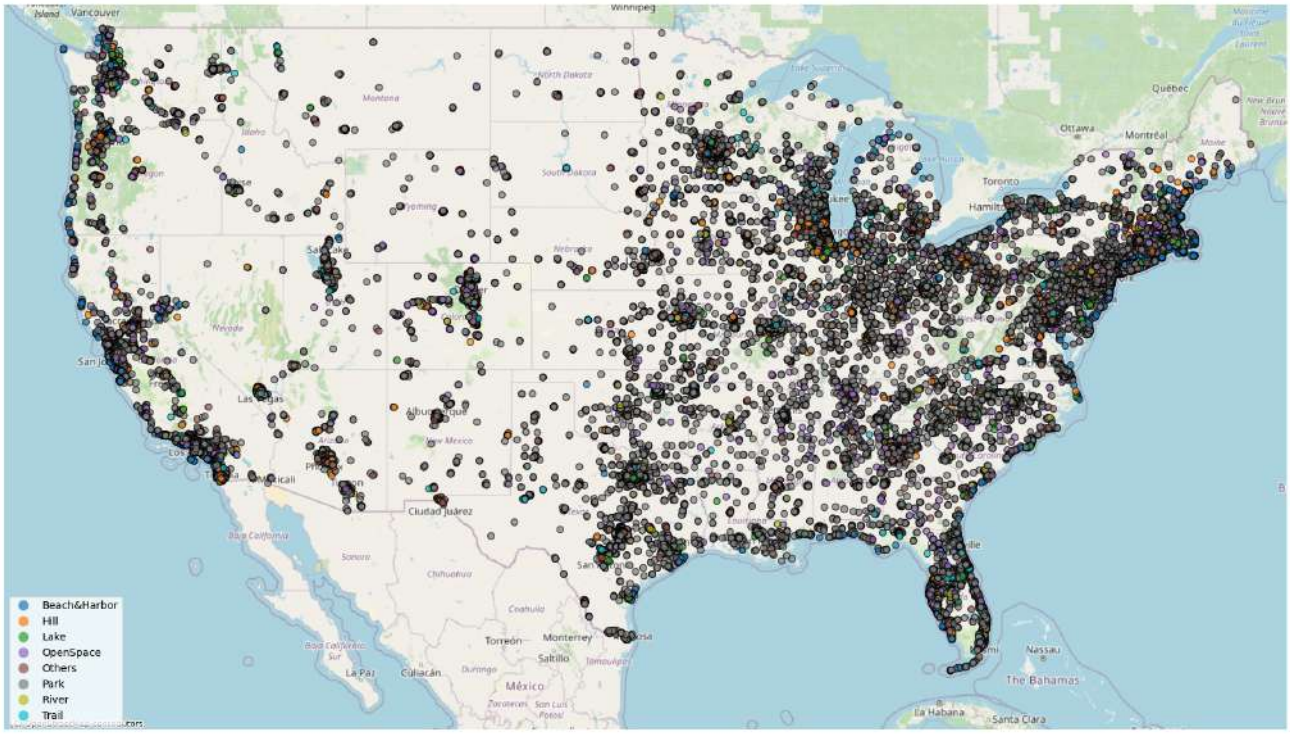

Notes: Figure 1 shows the distribution of water-based recreation sites from SafeGraph data. These sites are identified by intersecting the recreation site polygon from SafeGraph with the waterbody and flowline layers from the National Hydrography Dataset. We obtained 32,145 unique destinations from the SafeGraph data, out of which 21,131 (65.7%) are parks, 1,206 (3.8%) are river and lake sites, and 2,101 (6.5%) are open space. For additional details, see Section 2.

Figure 2. Temporal Variation of Recreation Visits and Water Quality

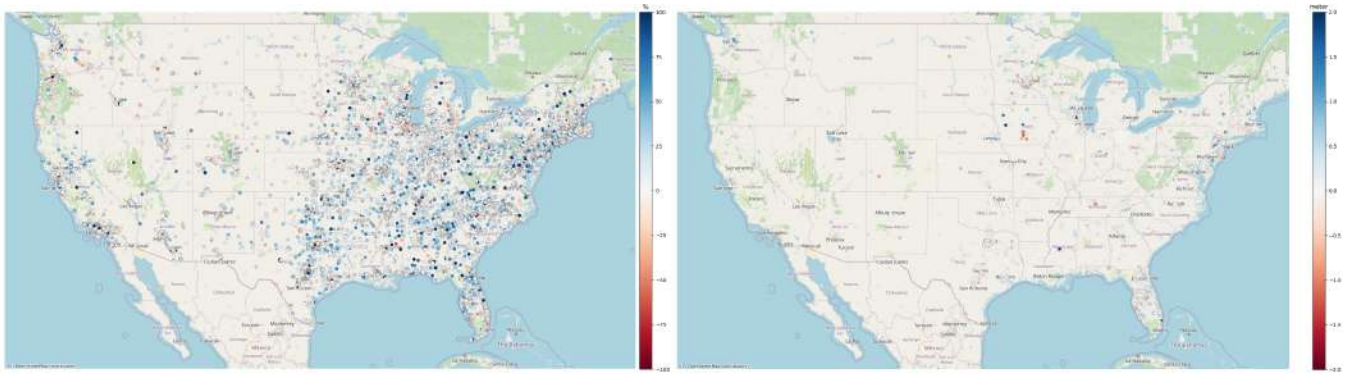

(**a**) Visit Changes (2018-2019)

(**b**) Secchi Depth Changes (2018-2019)

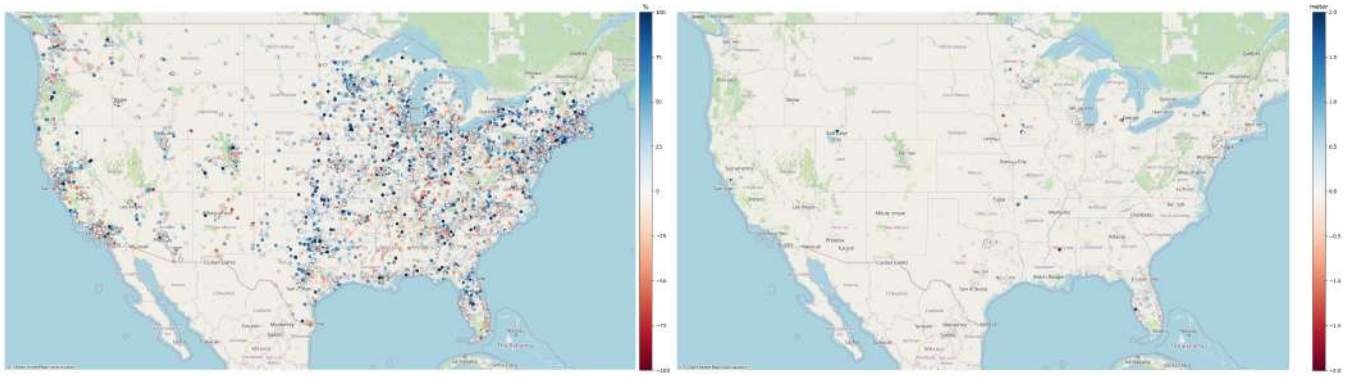

(**c**) Visit Changes (2019-2020)

(**d**) Secchi Depth Changes (2019-2020)

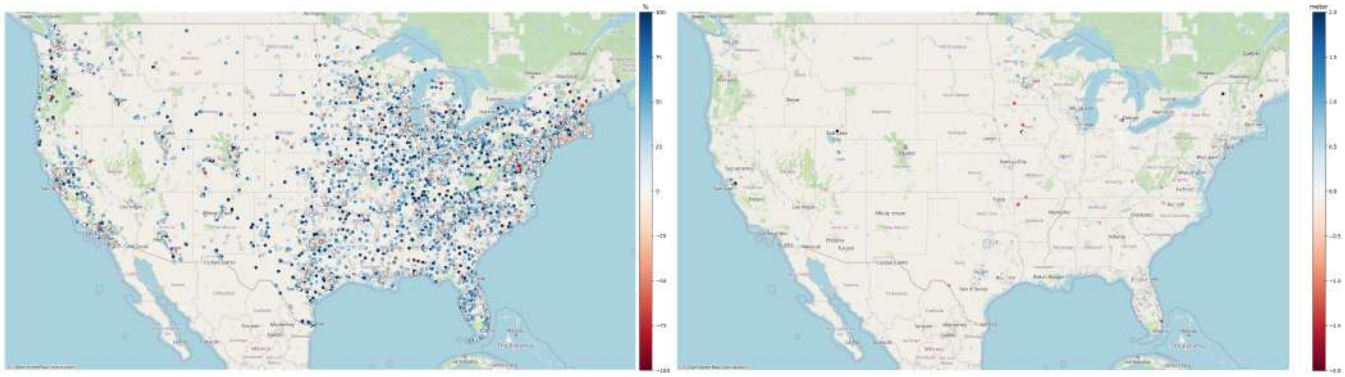

(**e**) Visit Changes (2020-2021)

(**f**) Secchi Depth Changes (2020-2021)

Notes: Figure 2 shows the temporal changes in recreation visits and water quality measures across sites. Figure 2a, 2c, and 2e show a decline in recreation visits in 2020 and then an increase in 2021. For additional details, see Section 2.

Figure 3. Spatial Variation of Recreation Visits and Water Quality

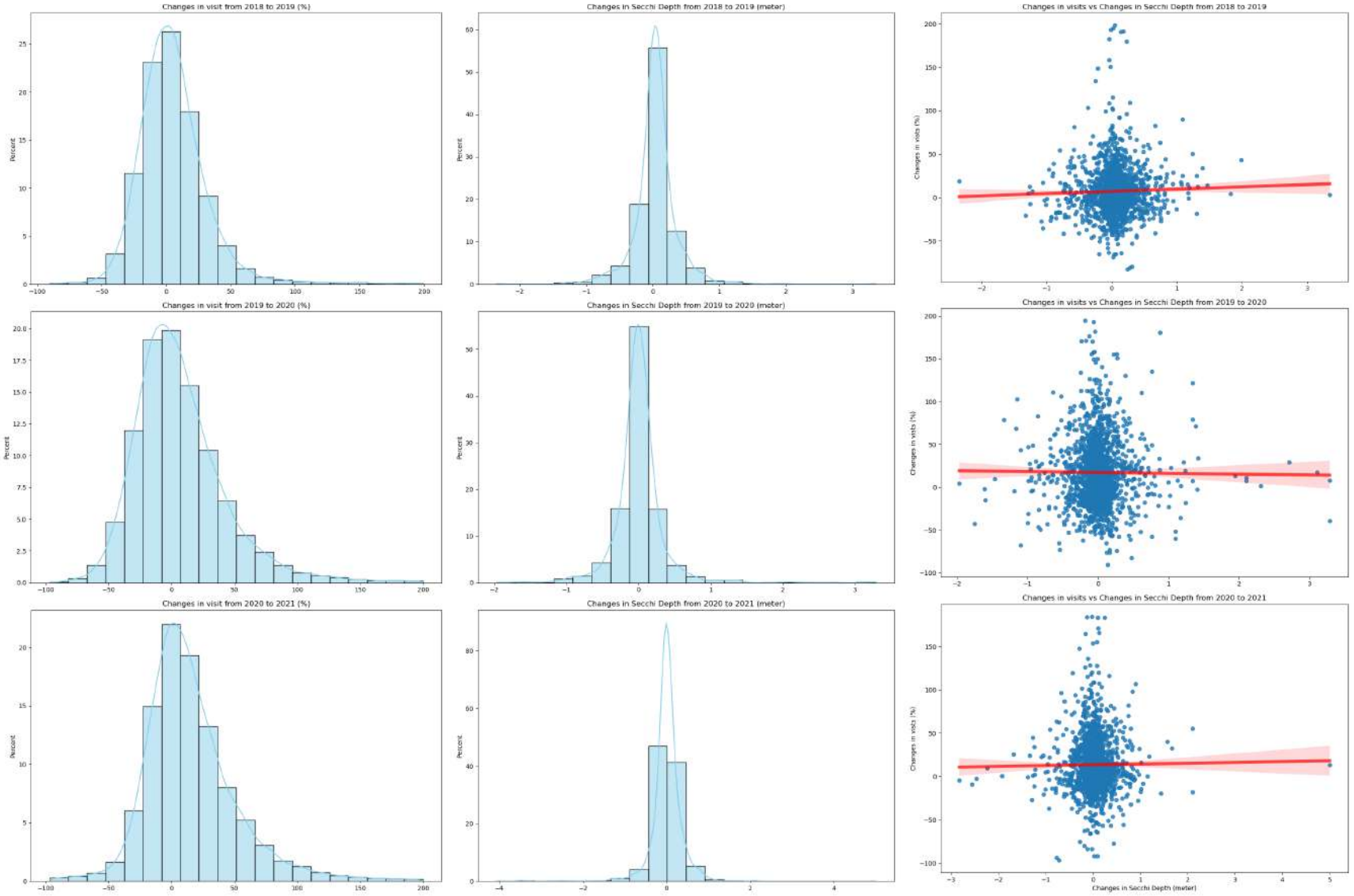

(**a**) Visit Changes (**b**) Secchi Depth Changes (**c**) Correlation

Notes: Figure 3 shows the spatial changes in recreation visits and water quality measures in our sample. For additional details, see Section 2.

I love that dirty water?
Value of water quality in recreation sites

Christopher R. Knittel, Jing Li, and Xibo Wan

Appendices for Online Publication

These appendices supplement our article "I love that dirty water? Value of water quality in recreation sites" with the following material:

- Online Appendix A includes additional details of spatial links across datasets, the spatial and temporal changes in average temperature, precipitation, and alternative water quality, and additional details of recreation visits and water quality measures.

- Online Appendix B contains details of data cleaning and imputation on water quality data

- Online Appendix C provides robustness checks on results from our preferred logit model.

Online Appendix A ADDITIONAL EVIDENCE

Online Appendix A.1 *Summary Statistics*

Table A1. Annual Recreation Visits by Site Type

	Count	2018	2019	2020	2021
Beach&Harbor	966	9879.50	10860.26	10605.56	11331.44
Hill	1,082	6096.41	8922.58	8384.85	8968.63
Open Space	2,101	7325.52	8976.90	8350.61	9234.63
Others	3,698	16920.54	21543.16	17206.60	20713.23
Trail	783	12195.62	15148.86	14033.27	13668.81
Lake	677	5967.72	6765.48	6818.39	7077.45
Park	21,131	6993.88	9830.34	9400.84	10480.21
River	529	7203.53	8313.50	8096.90	8391.82

Notes: Annual recreation visits and visitors in Safegraph sample from 2018 to 2021, averaged over site types. Device counts are normalized to the 2018 sample. For additional details, see Section 2.

Table A2. Summary Statistics of Recreation Sites by Water Quality Availability

	Count	Mean	S.D	Min	Max
Panel A: Sites with Secchi Depth Measures					
Travel Costs ($)	1,790	63.42	37.21	13.70	330.40
Travel Distance (mile)	1,790	44.61	26.83	8.35	209.71
Travel Time (h)	1,790	0.98	0.55	0.21	4.28
Area (Hectare)	1,790	422.12	1836.31	1.00	60180.64
Mean Temperature (C)	1,790	15.83	6.39	2.14	26.89
Precipitation (mm)	1,790	1217.60	394.00	142.40	3202.80
Panel B: Sites without Secchi Depth Measures					
Travel Costs ($)	30,355	53.23	34.92	10.74	436.48
Travel Distance (mile)	30,355	36.70	23.94	6.98	227.70
Travel Distance (mile)	30,355	0.80	0.50	0.13	5.46
Area (Hectare)	30,355	75.41	396.36	1.00	11055.82
Mean Temperature (C)	30,355	13.80	4.39	1.92	27.39
Precipitation (mm)	30,355	1109.30	457.54	39.10	3621.02

Notes: Table A2 show the means, standard deviations, minimums, and maximums for each variable in sites with and without Secchi depth measures. Travel costs are in CPI-deflated 2018 U.S. dollars. For additional details, see Section 2.

we follow several steps to match recreation sites with water bodies and water quality monitors. In the first step, we identify water-based recreation by intersecting the recreation site polygon with the waterbody and flowline layers from the National Hydrography Dataset. We define a site as a lake site as long as a site intersects with any water body and define a river site if a site only intersects with river flowlines. Figure A1a and A1a show how we process this matching.

In the second step, we introduce two methods to adjust the recreation site polygon to encompass the complete infrastructure and adjacent water bodies. For sites intersecting with small or medium lake water bodies, we union the recreation site polygon with adjacent lake water bodies and create the corresponding convex hull polygon as the adjusted polygon. Figure A2c presents the convex hull polygon of water-based recreation sites (denoted as brown). For sites intersecting with large lakes or rivers, we create a series of buffers of recreation site polygons to include the water bodies adjacent to a given site. Figure A2 gives an example of recreation site polygon adjustment. Figure A2d presents a 200-meter buffered polygon of water-based recreation sites (denoted as orange).

In the last step, we spatial join the adjusted site polygons with water quality monitors geo-locations and estimate the average water quality based on the available water quality measures within each site polygon.

Figure A1. Recreation Sites, Water Bodies, and Water Quality Monitors Matching

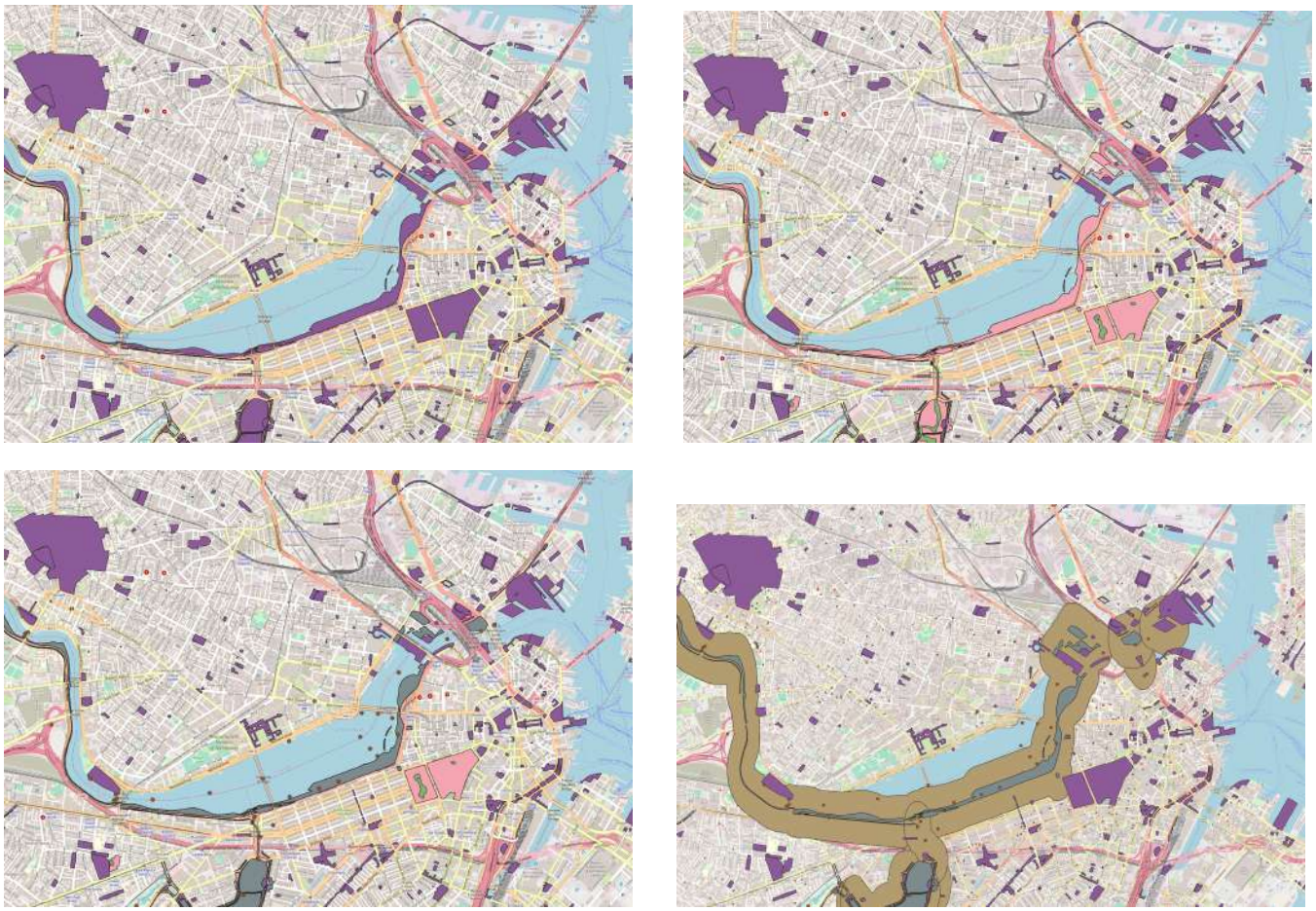

Notes: Figure A1 shows how we spatially match up recreation sites, water bodies, and water quality monitors. Figure A1a shows the recreation sites (denoted as purple) in Cambridge, Boston. Figure A1b plots the water-based recreation sites (denoted as pink) overlap with water bodies (denoted as green). Figure A1c presents the water-based recreation sites with water quality monitors (denoted as gray). Figure A1d depicts a 200-meter buffer for the water-based recreation sites with water quality monitors (denoted as brown). For additional details, see Section 2.

Figure A2. Adjustments on Recreation Sites Polygon

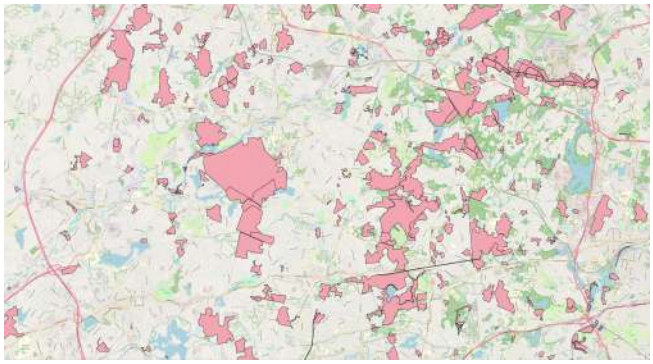

(**a**) Recreation Site Polygon

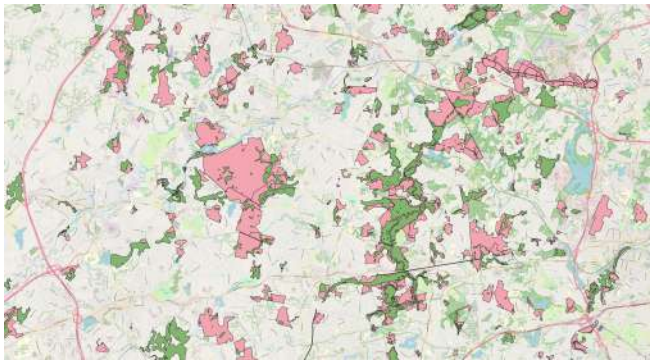

(**b**) Site Polygon and Water Bodies

(**c**) Convex Hull Polygon

(**d**) Buffer Polygon

Notes: Figure A2 shows how we adjust recreation sites' polygon based on the size and shape of water bodies. Figure A2a shows the raw recreation sites polygon from SafeGraph geometry data. Figure A2b plots the recreation site polygon (denoted as pink) and intersected water bodies (denoted as green). Figure A2c presents the convex hull polygon of water-based recreation sites (denoted as brown). Figure A2d presents the buffered polygon of water-based recreation sites (denoted as orange). For additional details, see Section 2.

Online Appendix A.3 *Cutoffs for Single Day Car-mode Trips*

Figure A3. Distribution of Travel Distance by Census Region

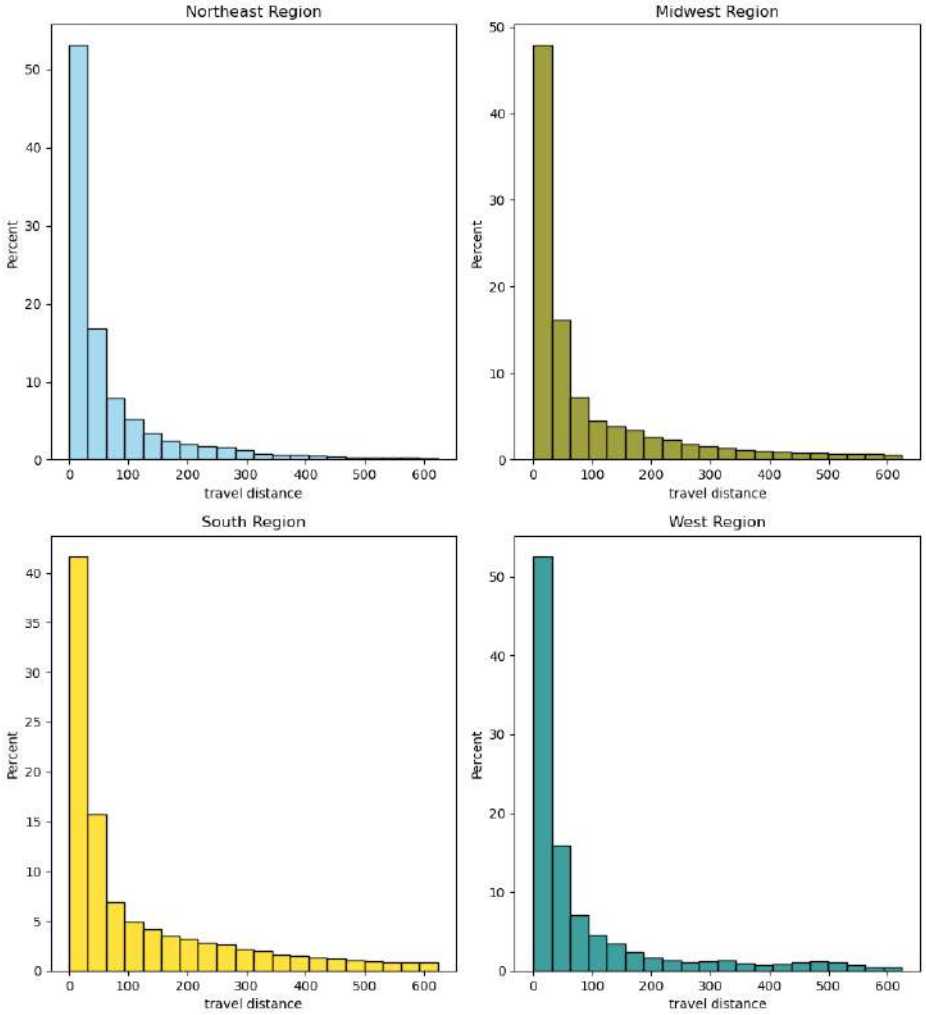

Notes: Figure A3 shows the distribution of travel distance from each origin to destination by census region in our sample. For visualization purposes, we restrict our sample to trips of which the travel distance is less than 85 percentile of the distribution. The Census region is based on the visitor's home location. We use a 300-mile travel distance as the cutoff to distinguish car-mode trips from flight-mode trips. For additional details, see Section 2.

Figure A4. Distribution of Travel Distance by State and Trip Mode

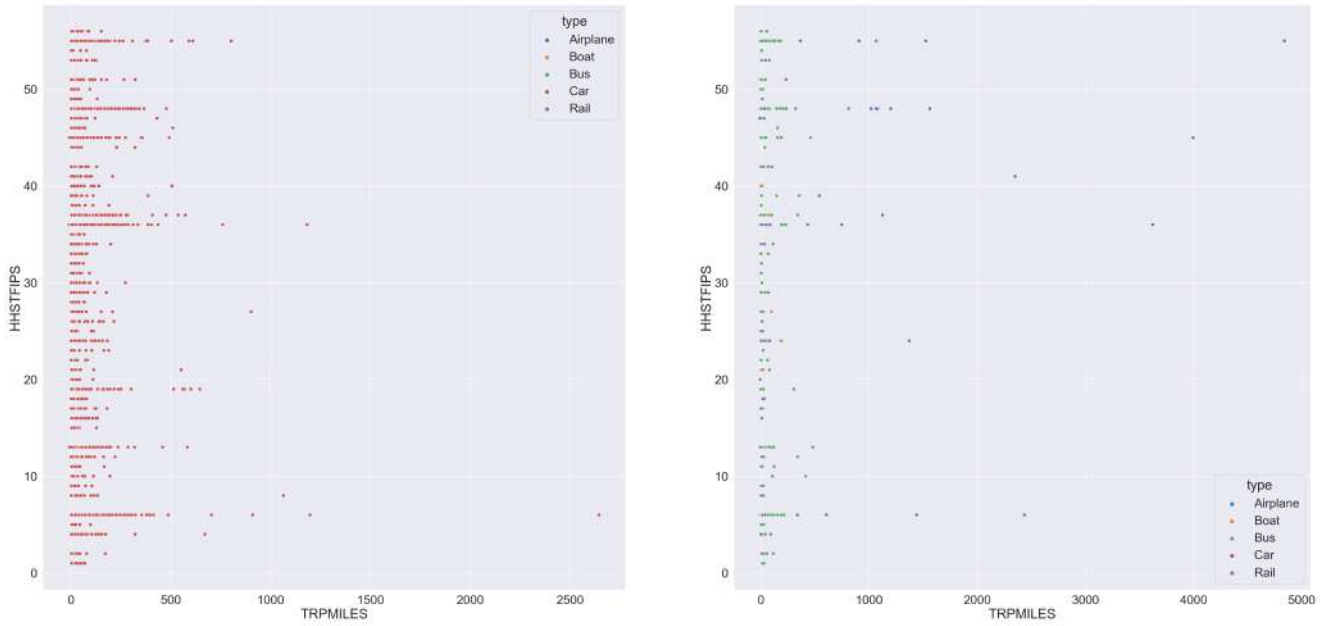

Notes: Figure A4 shows the distribution of travel distance by the state for car-mode and non-car-mode trips in the 2017 National Household Travel Survey. Figure A4a shows most car-mode trips are within a 300-mile distance. Figure A4b presents the distribution of travel distance by state and by trip mode. We find some evidence that flight-mode trips often travel more than 300 miles. For additional details, see Section 2.

Online Appendix A.4 *Statistics for Weather, Water Quality, and Recreation Visits*

Figure A5. Spatial Variation of Average Temperature and Precipitation

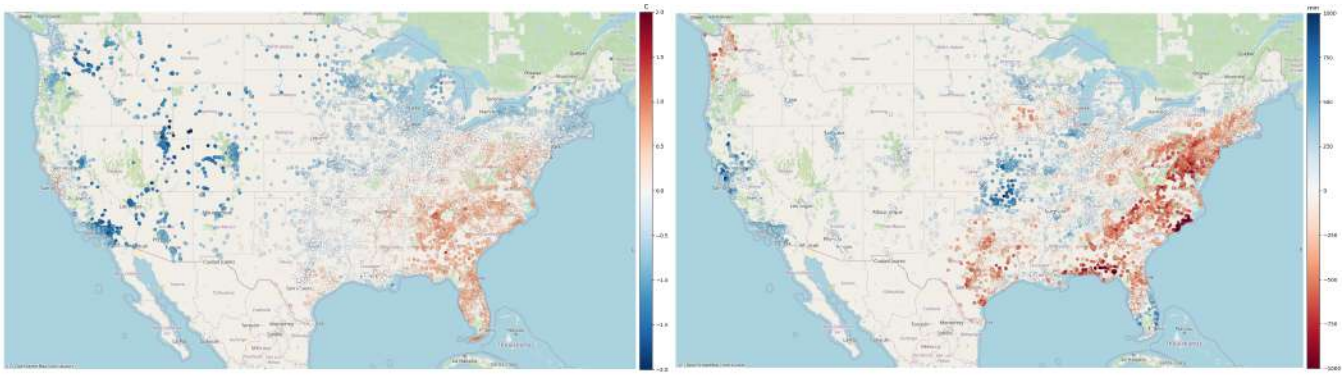

(**a**) Temperature Changes (2018-2019)

(**b**) Precipitation Changes (2018-2019)

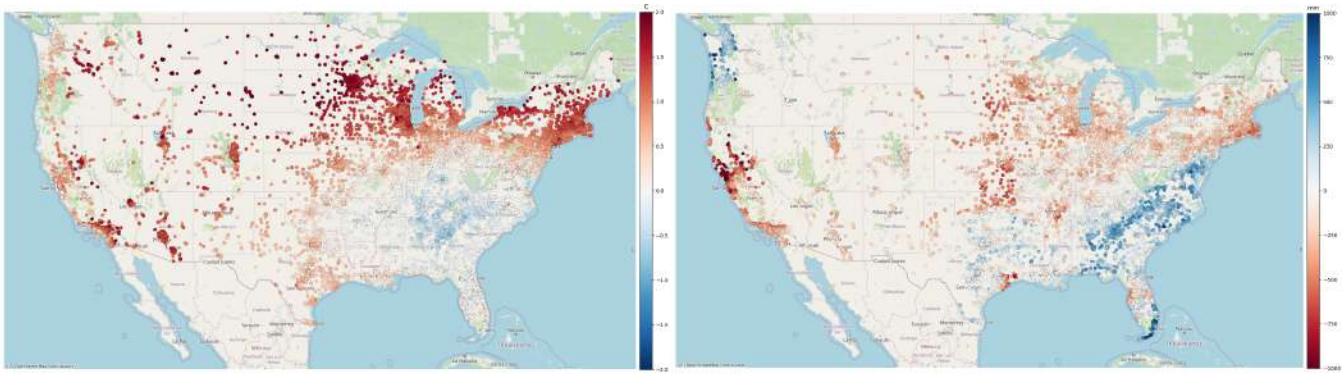

(**c**) Temperature Changes (2019-2020)

(**d**) Precipitation Changes (2019-2020)

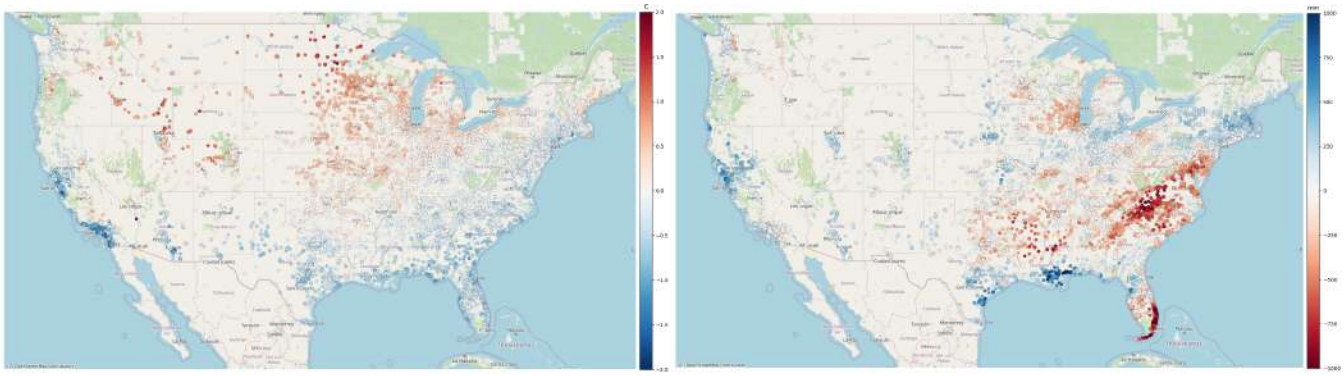

(**e**) Temperature Changes (2020-2021)

(**f**) Precipitation Changes (2020-2021)

Figure A6. Spatial Variation of Dissolved Oxygen and Chlorophyll-a

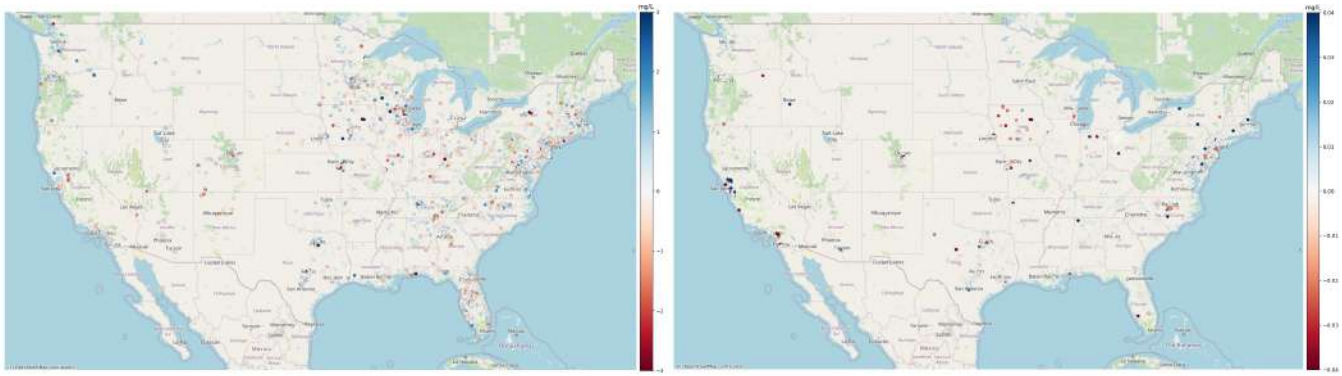

(**a**) Dissolved Oxygen Changes (2018-2019)

(**b**) Chlorophyll-a Changes (2018-2019)

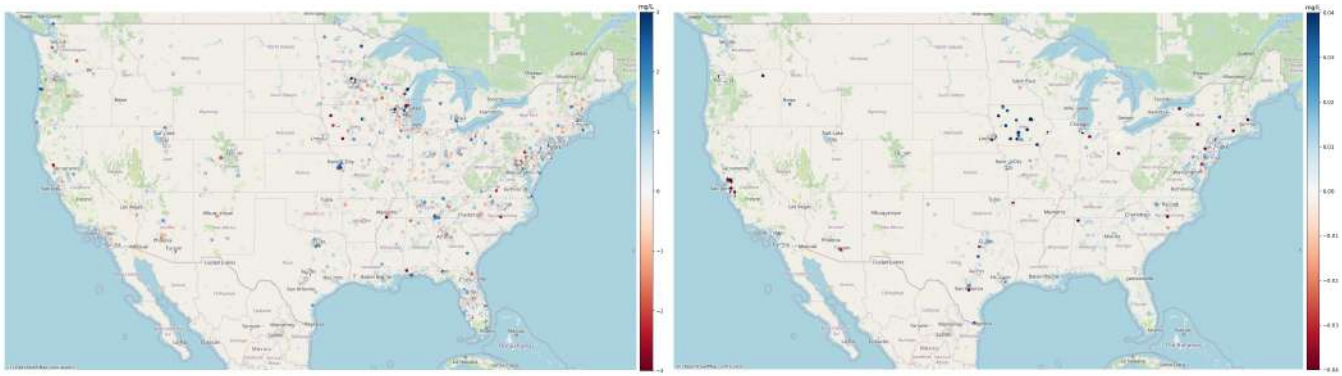

(**c**) Dissolved Oxygen Changes (2019-2020)

(**d**) Chlorophyll-a Changes (2019-2020)

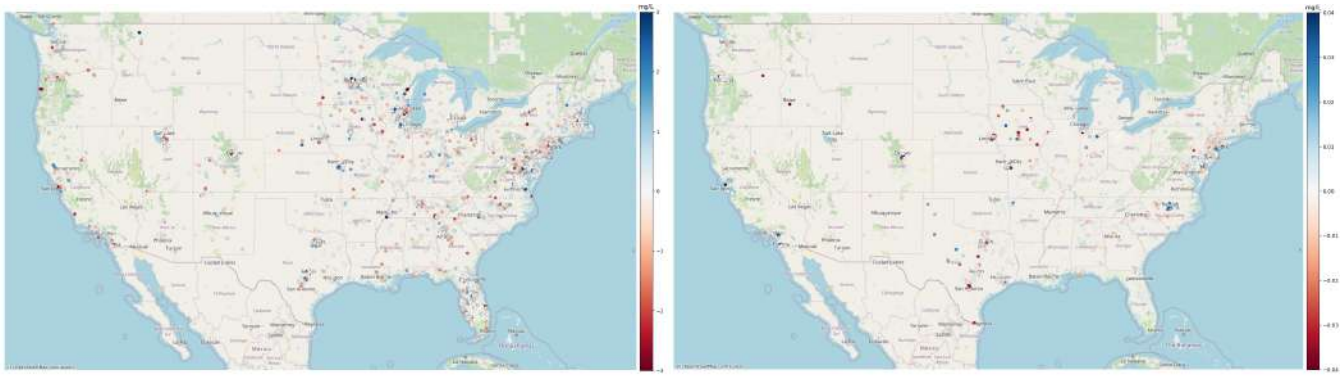

(**e**) Dissolved Oxygen Changes (2020-2021)

(**f**) Chlorophyll-a Changes (2020-2021)

Figure A7. Temporal Variation of Recreation Visits and Water Quality

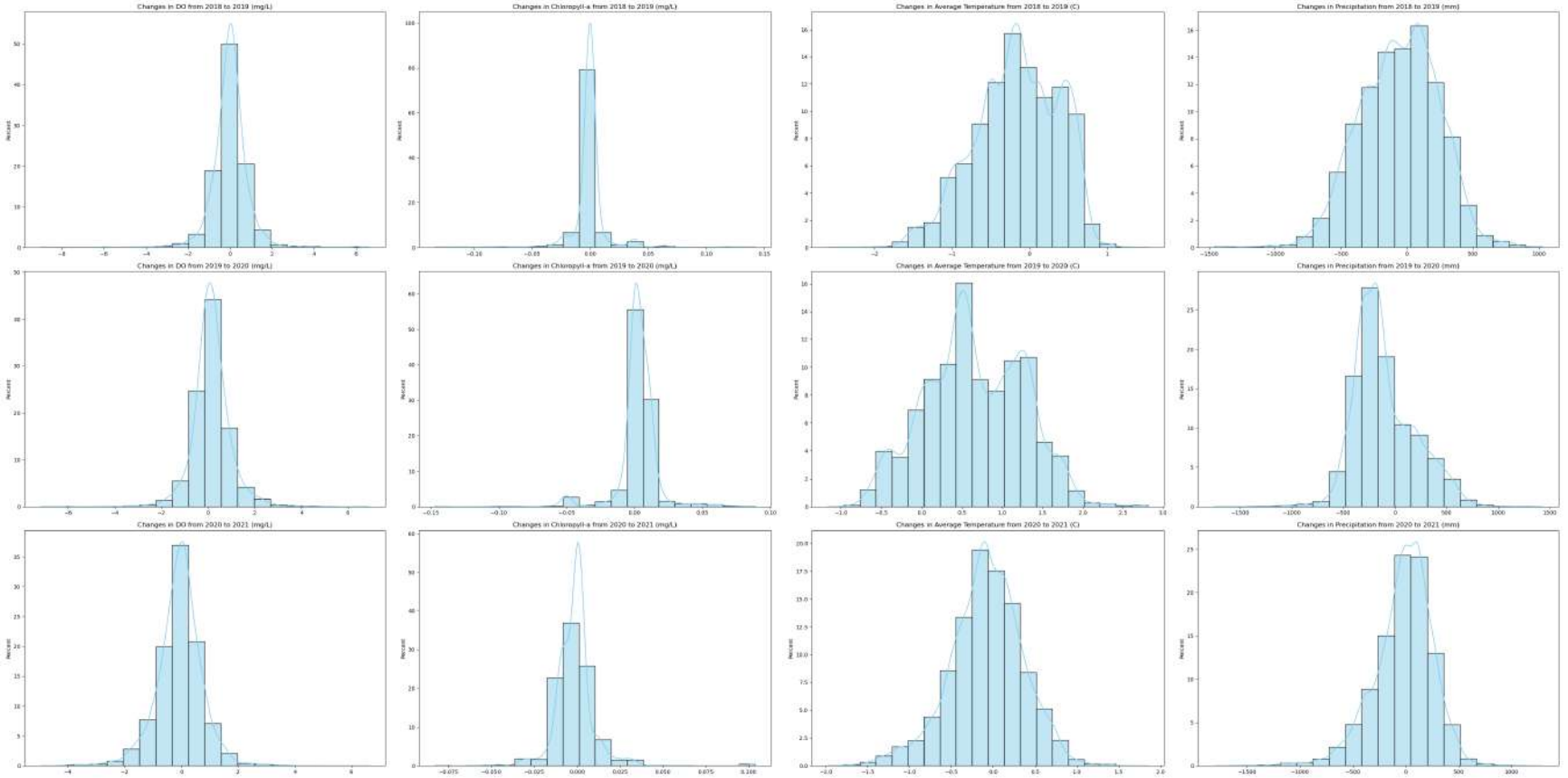

(**a**) Dissolved Oxygen (**b**) Chloropyll-a (**c**) Mean Temperature (**d**) Precipitation

Figure A8. Correlation between Recreation Visits and Water Quality

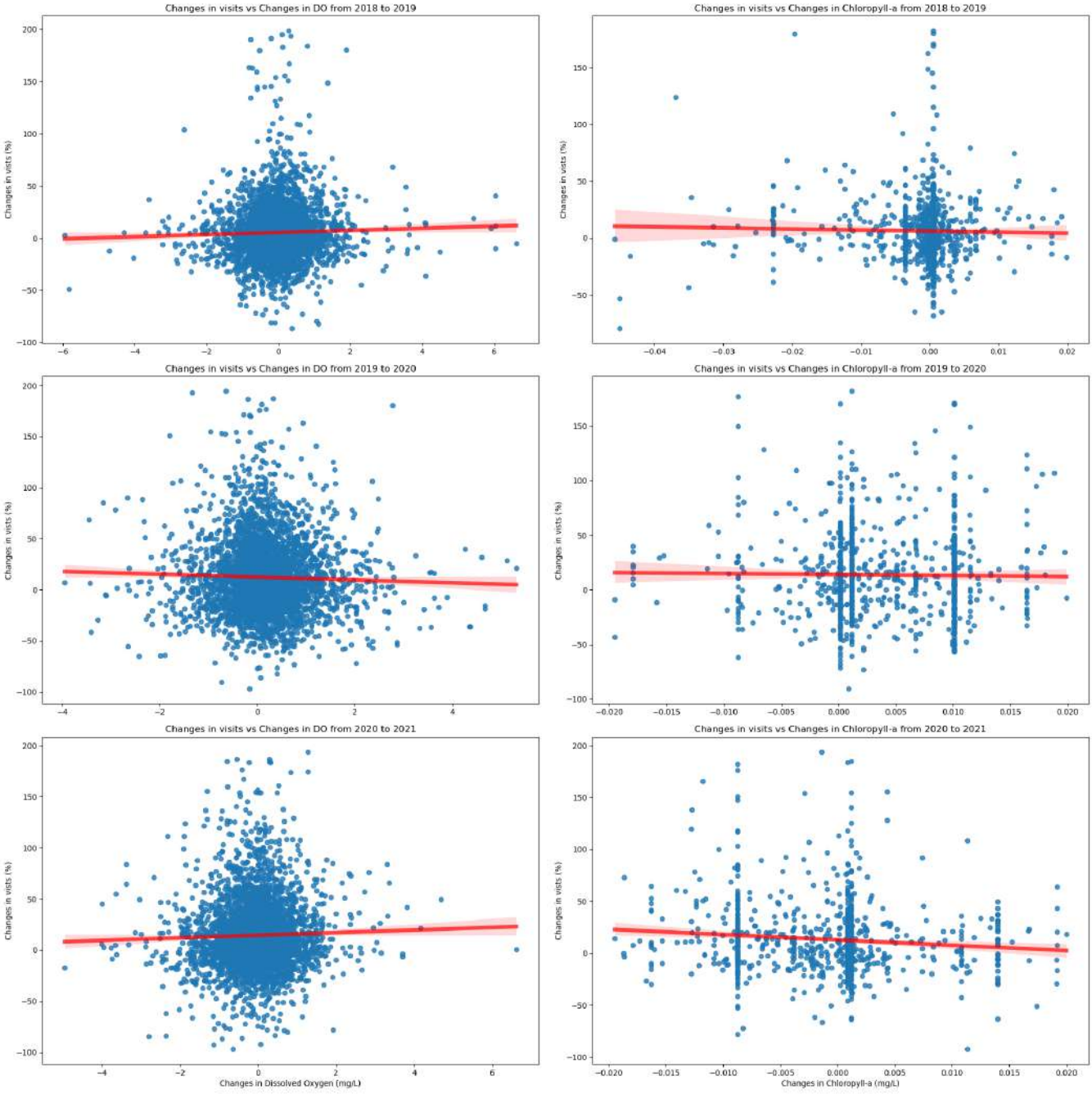

(**a**) Dissolved Oxygen Changes (**b**) Chlorophyll-a Changes

Online Appendix B WATER QUALITY DATA AND IMPUTATION

Online Appendix B.1 *Water Pollution Data*

Our analysis includes only rivers, streams, and lakes. This excludes estuaries, oceans, wells, pipes, canals, dams, and others that are not river or lake samples. Specifically, we limit the data to rivers/streams and lakes in a few steps. First, we restrict the sample media to surface water, which removes typically less than 1 percent of records that are coded as other media subtypes such as effluent or groundwater. Next, we limit the type to lake, reservoir, impoundment, or stream[28].

We use the characteristic name to filter out our main water quality measures. A single characteristic name often corresponds to multiple parameter codes. The EPA concordance provides the meaning of parameter codes, including information on sample preparation (e.g., details regarding filter size), whether the measurement was in the field or laboratory, measurement units, result sample fraction (e.g., total versus dissolved), result statistical basis (e.g., mean, median), and additional measurement method details. See more details on the Water Quality Portal website. For dissolved oxygen, we collect water quality data under "Dissolved oxygen" and "Dissolved oxygen (DO)". For Secchi Depth, we collect data under name of "Secchi depth", "Depth, Secchi disk depth", "Depth, Secchi disk depth (choice list)", and "Secchi Reading Condition (choice list)". For Chlorophyll-a, we collect data under name of "Chlorophyll a" and "Chlorophyll A".

We impose several sample exclusions. We drop observations with missing observation dates, latitude, and longitude, and outside the continental U.S. We limit to latitude and longitude observations that are located within a U.S. county. We also limit analysis to ambient monitoring. To limit the influence of outliers, for each reading above the 99th percentile of the distribution of readings, separately by pollutant, we recode the result to equal the 99th percentile. For all pollutants, we keep all records with unit data that are easily converted to standard units. In our data, the tuple of a station's name, the name of the agency that manages it, and the repository uniquely identify a station. We use longitude and latitude to define monitoring sites given the fact that monitors from different repositories could potentially have the same longitude and latitude. Next, we do not account for reading depth since many depth values have missing units. Finally, to make the most of the data from the water quality portal, we extract any letter from the results such as B, C, I, J, K, L, M, N, O, P, T, U, W, Z, and $ to get clean numeric measures on water quality.

[28]We consider a monitor as river monitor if the type is "river", any type containing "river", "stream", and any type containing "stream". We consider a monitor as a lake monitor if the type is "Lake, Reservoir, Impoundment, or pond".

Online Appendix B.2 *Water Quality Imputation*

One of the challenges in this study is represented by the high percentage of missing data (between 60% and 80%) and the high temporal and spatial variability that characterizes the water quality variables. We considered machine learning techniques to impute our water quality measures from EPA's water quality portal. After imputation, we spatial join the water quality monitors with adjusted site polygon and then take the average of water quality measures within each recreation site polygon as our water quality measures for a site. Appendix Figure A1d provides an example of adjusted recreation site polygons in Cambridge, Boston.

Specifically, the competing algorithms implement Mean imputation, Bayesian Ridge (BR)[29], Decision Tree Regressor (DT)[30], Multivariate Imputation by Chained Equations (MICE)[31], and K-nearest neighbors Regressor (KNN)[32]. After imputing the data, we use Random Forest Regressor to test the accuracy of the imputed data[33]. We use scikit-learn to implement the above algorithms. We consider 12 missing data scenarios for the data imputation. Rubin (1976) classified missing data problems into three categories. In his theory, every data point has some likelihood of being missing. The process that governs these probabilities is called the missing data mechanism or response mechanism. If the probability of being missing is the same for all cases, then the data are said to be missing completely at random (MCAR), which is often unrealistic for the data at hand. If the probability of being missing is the same only within groups defined by the observed data, then the data are missing at random (MAR). Modern missing data methods generally start from the MAR assumption. MCAR is often unrealistic for the data at hand. If neither MCAR nor MAR holds, then we speak of missing not at random (MNAR). Strategies to handle MNAR are to find more data about the causes for the missingness, or to perform what-if analyses to see how sensitive the results are under various scenarios. We also consider 4 types of missing data fractions (20%, 40%, 60%, and 80%) to better understand how these algorithms perform under each scenario.

The analysis proceeds in the following three steps. First, the dataset was pre-processed before any analysis

[29] It is an estimator that assumes and predicts the target by calculating its probability distribution during training. This method can cope with data sparsity more effectively than other methods.

[30] It is a regressor that predicts the value of a target variable by learning simple decision rules inferred from the data features.

[31] it is a robust, informative method of dealing with missing data in datasets. The procedure 'fills in' (imputes) missing data in a dataset through an iterative series of predictive models. In each iteration, each specified variable in the dataset is imputed using the other variables in the dataset. These iterations should be run until it appears that convergence has been met.

[32] It is a regressor that calculates the distance (using all variables) from the target point to the others and makes a prediction by interpolating the nearest neighbors in the dataset.

[33] Random Forest is an ensemble learning method for classification, regression, and other tasks that operates by constructing a multitude of decision trees at training time. For classification tasks, the output of the random forest is the class selected by most trees. For regression tasks, the mean or average prediction of the individual trees is returned.

to deal with the different units, orders of magnitude, not unified variable names, and different sampling frequencies. Second, we assess each selected imputation model, calculate their loss functions, and conduct cross-validation to compute the Nash-Sutcliffe efficiency (NSE).

$$NSE = 1 - \frac{\sum_{i=1}^{n}(x_i^0 - x_i^c)^2}{\sum_{i=1}^{n}(x_i^0 - \overline{x_i^0})^2} \tag{B1}$$

where x_i^0 is the ith observed value, x_i^c is the ith imputed value, $\overline{x_i^0}$ is the mean of observed values. NSE varies between -∞ and 1. If NSE is 1, the imputed values match the records perfectly. If NSE is 0, the imputed values are as good as the observation mean. If NSE is negative, the observation mean is a better predictor than imputed values. Therefore, higher NSE values are desirable since they indicate a more accurate imputation model; For chemical water quality measure, we think the imputation result is very good if NSE larger than 0.65; good if NSE is between 0.5 and 0.65; satisfactory if NSE is between 0.35 and 0.5; and unsatisfactory if NSE is less than 0.35.

The dataset consists of 44,869 time series (11 years × 4,079 monitoring stations) for Dissolved Oxygen, 33,165 time series (11 years × 3,015 monitoring stations) for Secchi Depth, 5,687 time series (11 years × 517 monitoring stations) for Chlorophyll-a. To evaluate the performance of the different imputation models adopted and to choose the best one for each feature, k-fold cross-validation with k = 10 was used in this study. The dataset was min-max normalized before any analysis to deal with the different units and orders of magnitude. The best models were the ones with the optimal hyper-parameters.

Figure B1 shows the results of Secchi depth for each model under 12 missing data scenarios. Overall, the imputation performance is adequate except for MICE. Among these methods, the NSE varies from 0.35-0.6 across missing data patterns and missing data fractions. KNN (neighbor=3/4/5) shows very good performance when the percentage of missing data is small and performs good when the percentage is large. Similarly, in Figure B2, the performance of Dissolved Oxygen imputation is between Satisfactory and very good across missing data patterns and missing data fractions. In contrast, in Figure B3, the NSE of Chlorophyll-a impuation is around 0.4 when the percentage of missing data is small and performs unsatisfactory when the percentage is large, suggesting these algorithms might not impute the missing value very well in Chlorophyll-a measure. Given the performance of imputation on each water quality measure and the percentage of missing data in our sample, We use the KNN regressor with 5 neighbors as our best model to impute the Secchi depth and dissolved oxygen data. We will only use the buffer method to calculate the average Chlorophyll-a measure.

Figure B1. Water Quality Imputation on Secchi Depth

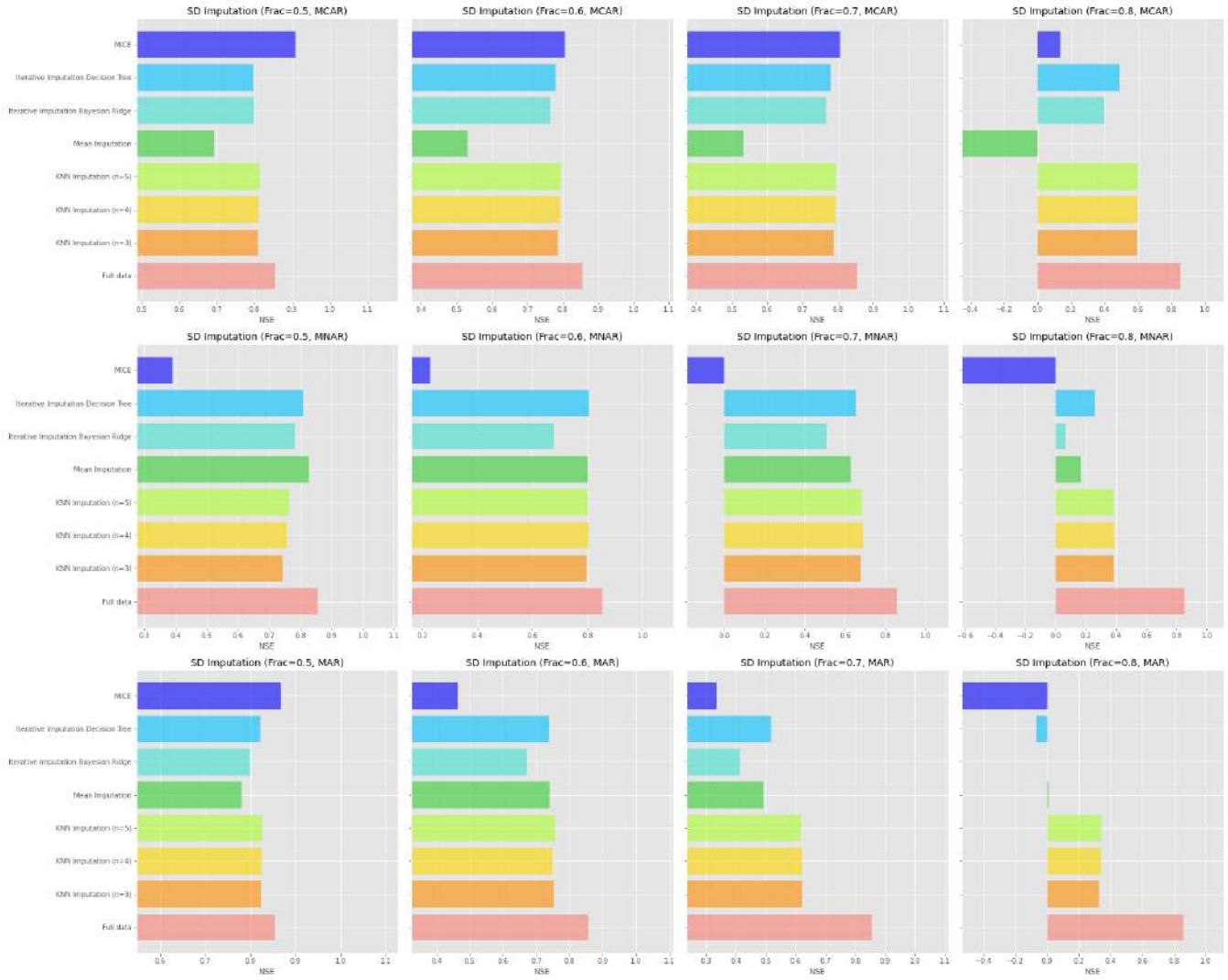

Notes: Figure B1 shows NSE scores of Secchi Depth using machine learning algorithms. We consider 12 missing data scenarios (3 missing data patterns and 4 missing data fractions). We use Nash-Sutcliffe efficiency (NSE) to evaluate the performance of the imputation results. For additional details, see **Online Appendix B.2**.

Figure B2. Water Quality Imputation on Dissolved Oxygen

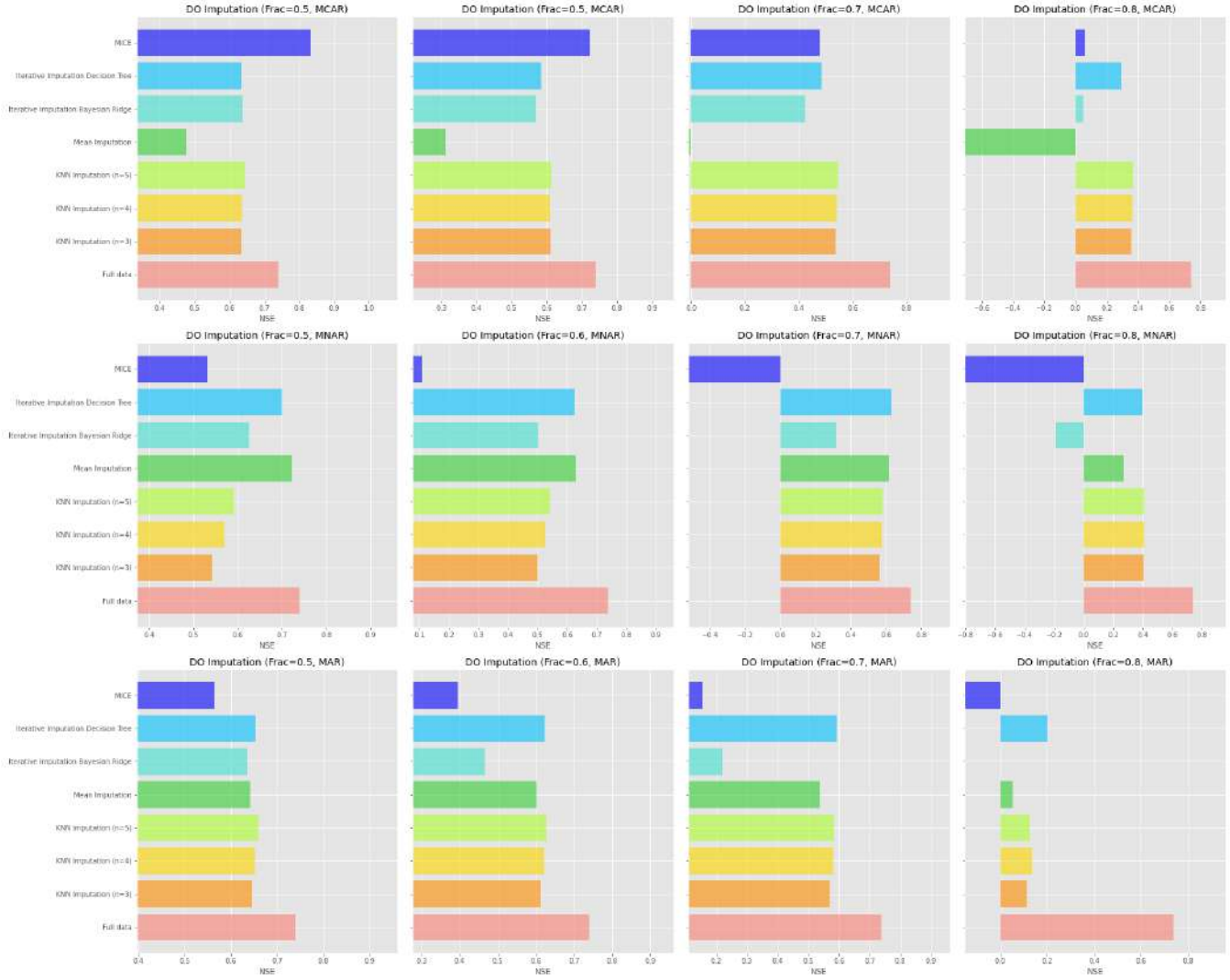

Notes: Figure B2 shows NSE scores of Dissolved Oxygen using machine learning algorithms. We consider 12 missing data scenarios (3 missing data patterns and 4 missing data fractions). We use Nash-Sutcliffe efficiency (NSE) to evaluate the performance of the imputation results. For additional details, see **Online Appendix B.2**.

Figure B3. Water Quality Imputation on Chlorophyll-a

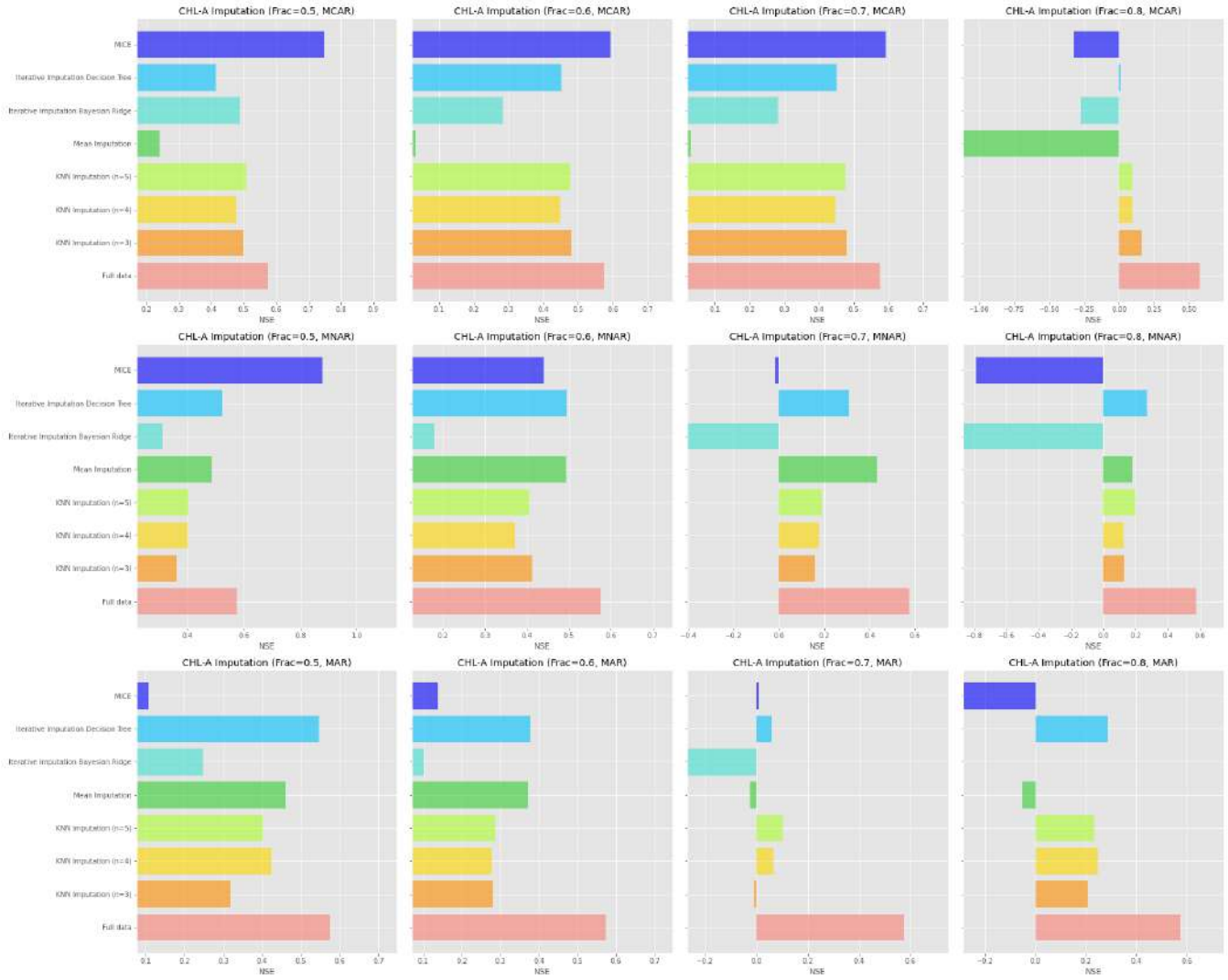

Notes: Figure B3 shows NSE scores of Chlorophyll-a using machine learning algorithms. We consider 12 missing data scenarios (3 missing data patterns and 4 missing data fractions). We use Nash-Sutcliffe efficiency (NSE) to evaluate the performance of the imputation results. For additional details, see **Online Appendix B.2**.

Online Appendix B.3 *Satellite Estimate of Water Quality Measures*

A growing literature has been mapping the water quality parameters using satellite images over inland lakes (Barrett and Frazier (2016); Chandrasekar et al. (2010); Liu et al. (2017); Molkov et al. (2019); Olmanson et al. (2008); Pahlevan et al. (2017); Potes et al. (2011, 2012, 2018); Toming et al. (2016)), while most of them focus on certain lakes or regions. In this section, we explore reliable remote sensing methods for the spatial and temporal cover of water quality parameters to provide an additional view of water quality. Specifically, we develop the Secchi depth measurements by applying the quasi-analytic algorithm by Lee et al. (2016) to data from the Sentinel-2 mission (Multi-Spectral Instrument (MSI)). This algorithm has shown promise in lakes as well as coastal waters (Merrill et al. (2022)).

The Sentinel-2 mission consists of a constellation of two polar-orbiting satellites, Sentinel-2A and Sentinel-2B, each one equipped with an optical imaging sensor (MSI). Sentinel-2A was launched on 23 June 2015 and Sentinel-2B followed on 7 March 2017. These twin polar-orbiting satellites allow a high 2-3 days revisit time for Alqueva reservoir since July 2017. MSI data are acquired in 13 spectral bands in the visible and near-infrared and have very high spatial resolution, with three bands at 60 m, six bands at 20 m and four bands at 10 m. The dataset used in this study is the Sentinel-2 Level-1A product, in which spectral reflectances have been atmospherically corrected through the Sen2Cor algorithm.

We follow several steps to derive the Secchi depth measurements. First, we derive K_d^{tr} from Sentinel-2 images. Second, following the new underwater visibility theory, the Secchi-disk depth is inversely proportional to the diffuse attenuation coefficient and can be expressed (Lee et al., 2015a)

$$Z_{SD} = \frac{1}{2.5Min(K_d^{tr})} ln(\frac{|0.14 - R_r^{tr}s|}{0.013}) \tag{B1}$$

where K_d^{tr} is the diffuse attenuation coefficient at the transparent window of the water body within the visible domain (410–665 nm), $R_r^{tr}s$ is the remote-sensing reflectance corresponding to this wavelength. Finally, we use the in-situ measurements from Water quality portal to validate the Secchi depth measurements we derived from satellite images. See more details in Lee et al. (2016). Appendix Figure B4 and B4 shows a strong correlation between estimated Secchi depth and in-situ water quality measures.

Figure B4. Validation on Secchi Depth Measurements using Raw Data

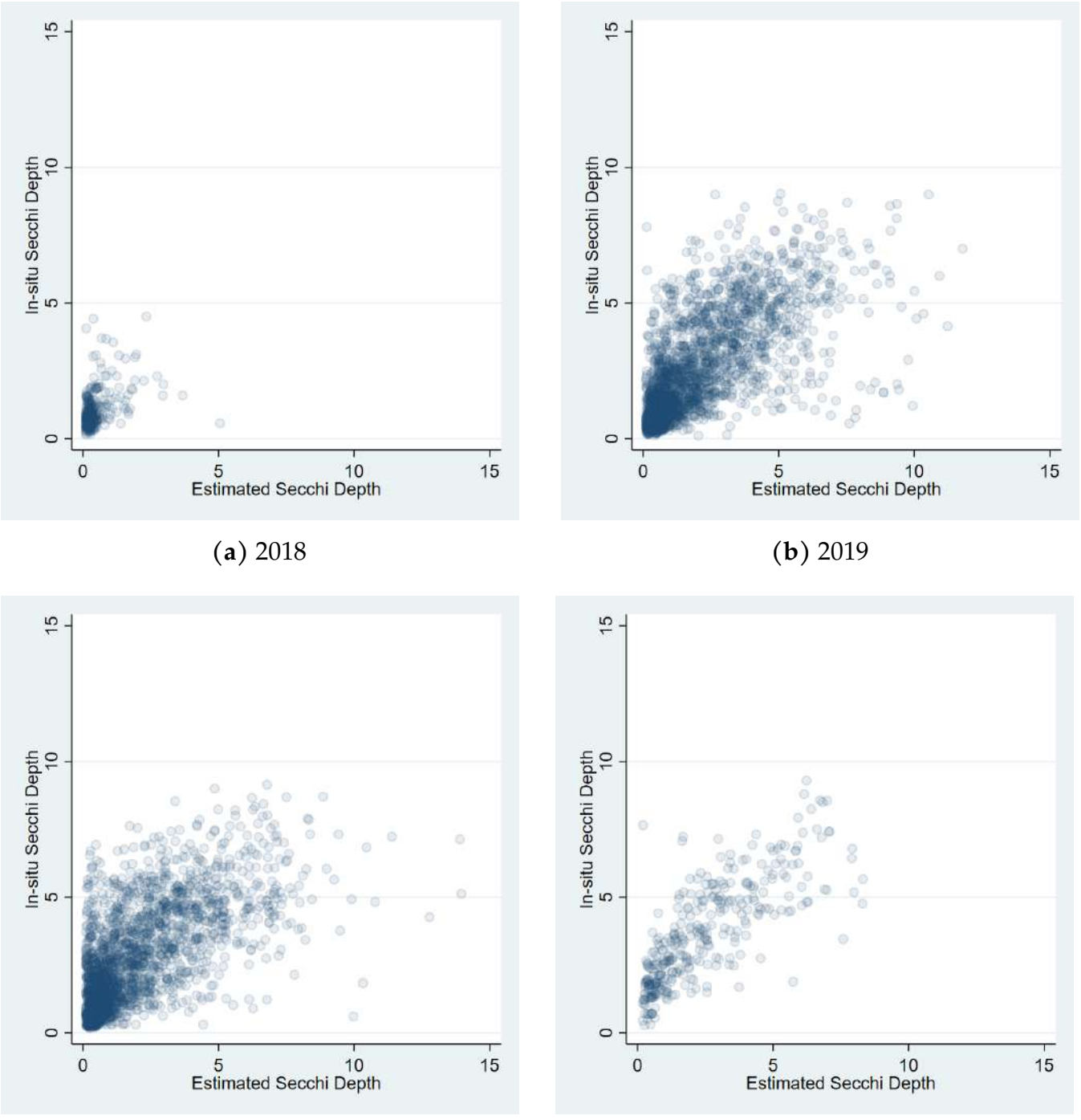

(**a**) 2018

(**b**) 2019

(**c**) 2020

(**d**) 2021

Notes: Figure B4 shows validation results using derived Secchi depth from Sentinel-2A images and raw water quality data from the water quality portal. For additional details, see Section 2.

Figure B5. Validation on Secchi Depth Measurements using Imputed data

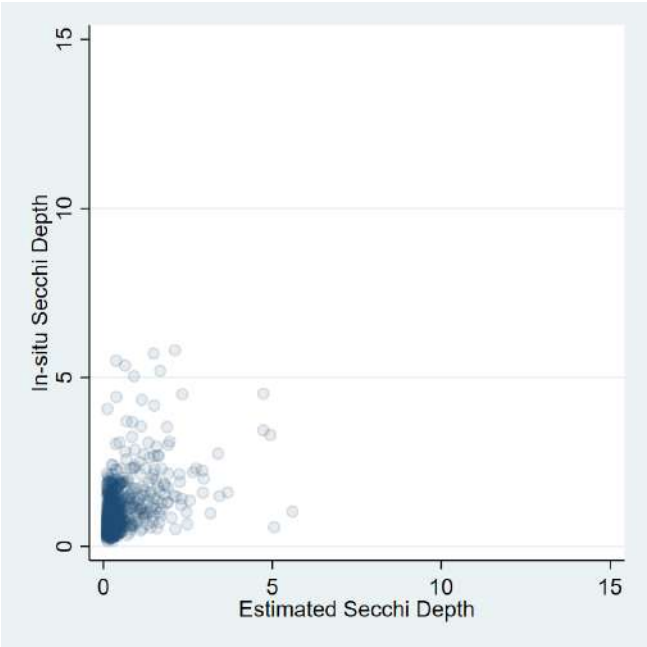

(**a**) 2018

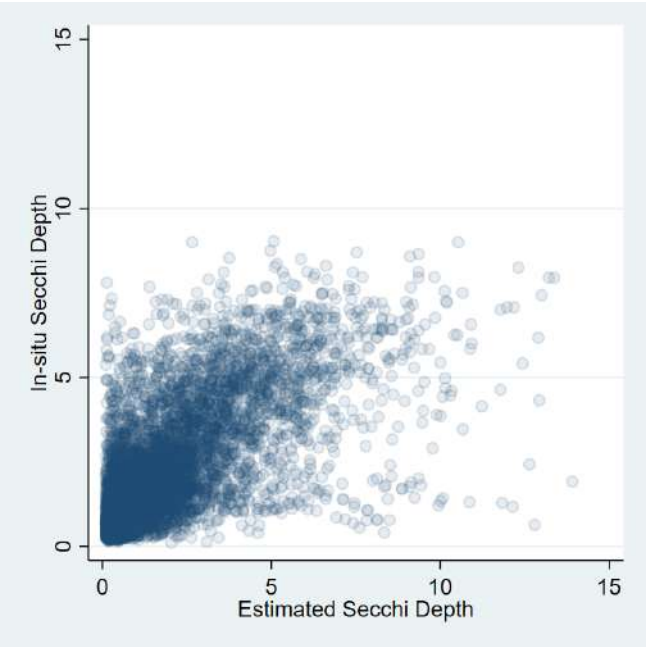

(**b**) 2019

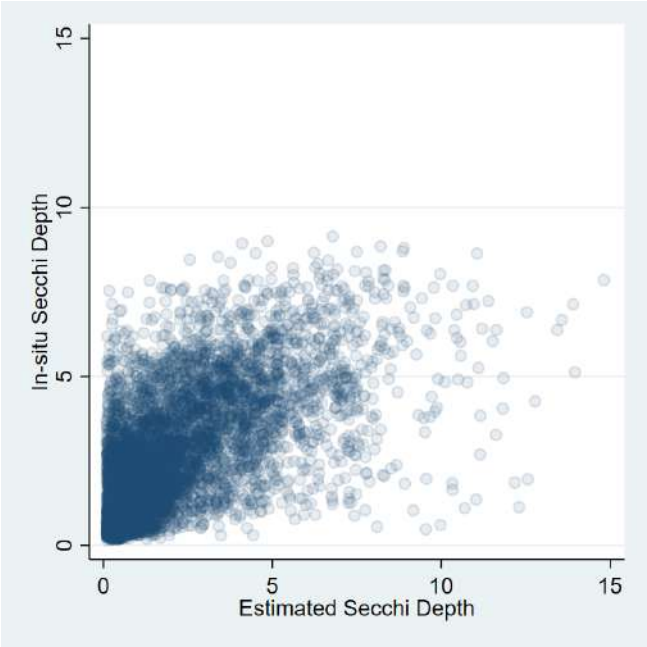

(**c**) 2020

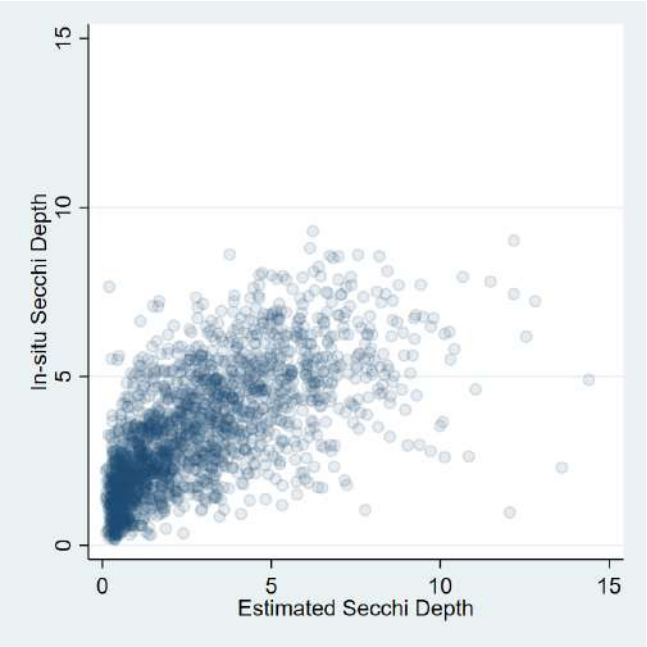

(**d**) 2021

Notes: Figure B5 shows validation results using derived Secchi depth from Sentinel-2A images and raw water quality data from the water quality portal. For additional details, see Section 2.

Online Appendix C ROBUSTNESS CHECKS AND SENSITIVITY TESTS

Table C1. Robustness Checks: Alternative Recreation Site Buffer

	(1)	(2)	(3)	(4)	(5)
Travel Costs	-0.004***	-0.004***	-0.004***	-0.004***	-0.004***
	(0.000)	(0.000)	(0.000)	(0.000)	(0.000)
COVID	0.196***	0.193***	0.200***	0.215***	0.217***
	(0.010)	(0.010)	(0.009)	(0.009)	(0.009)
Secchi Depth	0.004*	0.010***	0.010***	0.012***	0.011***
	(0.002)	(0.002)	(0.002)	(0.002)	(0.002)
Secchi Depth X COVID	0.006***	-0.000	-0.002**	-0.003***	-0.003***
	(0.001)	(0.001)	(0.001)	(0.001)	(0.001)
ln(Cumu. Cases)	-0.002***	-0.002***	-0.002***	-0.002***	-0.003***
	(0.000)	(0.000)	(0.000)	(0.000)	(0.000)
Lockdown Dummy	0.013*	0.022***	0.018**	0.018**	0.027***
	(0.008)	(0.007)	(0.007)	(0.007)	(0.007)
Observations	2503106	2819946	3002282	3206806	3362367
N(BlockGroup)	149974	155145	156899	158763	160905
CBG FEs	Yes	Yes	Yes	Yes	Yes
Site FEs	Yes	Yes	Yes	Yes	Yes
Weather FEs	Yes	Yes	Yes	Yes	Yes
MWTP	0.967	2.572	2.631	3.311	3.033
Buffer	100m	200m	300m	400m	500m

Notes: Table C1 shows the results of running the recreation demand model using alternative polygon buffers. The standard error is clustered at CBG level. Robust standard errors are in parentheses. ***,**,* denotes statistical significance at the 1%, 5%, and 10% levels, respectively. For additional details, see Section 4.

Table C2. Robustness Checks: Alternative Definition of Travel Costs

	(1)	(2)	(3)	(4)
Travel Costs	-0.004***	-0.004***	-0.006***	-0.002***
	(0.000)	(0.000)	(0.000)	(0.000)
Secchi Depth	0.010***	0.010***	0.007***	0.012***
	(0.002)	(0.002)	(0.002)	(0.002)
COVID	0.194***	0.220***	0.186***	0.203***
	(0.010)	(0.011)	(0.009)	(0.010)
Secchi Depth X COVID	-0.000	0.001	-0.000	0.000
	(0.001)	(0.001)	(0.001)	(0.001)
ln(Cumu. Cases)	-0.002***	-0.004***	-0.001***	-0.002***
	(0.000)	(0.000)	(0.000)	(0.000)
Lockdown Dummy	0.022***	0.035***	0.022***	0.022***
	(0.007)	(0.008)	(0.007)	(0.007)
Observations	2819946	2041946	2867391	2819946
N(BlockGroup)	155145	120906	157849	155145
CBG FEs	Yes	Yes	Yes	Yes
Site FEs	Yes	Yes	Yes	Yes
Weather FEs	Yes	Yes	Yes	Yes
MWTP	2.551	2.529	1.245	5.531
Definition	Oper.+ 1/3Oppo.	Oper.+ 1/3Oppo.	Oper.	Oper.+ Oppo.

Notes: Table C2 shows the results of running the recreation demand model using alternative definitions of travel costs. All specifications include site and CBG fixed effects, and weather controls. Column 1 uses CPI-Deflated operation costs and one-third of the value of travel time ($2018); column 2 uses actual operation costs and one-third of the value of travel time; column 3 only includes CPI-Deflated operation costs ($2018); column 4 uses operation costs and full value of travel time. The standard error is clustered at the CBG level. Robust standard errors are in parentheses. ***,**,* denotes statistical significance at the 1%, 5%, and 10% levels, respectively. For additional details, see Section 4.

Table C3. Robustness Checks: Alternative Car-mode Trip Cutoffs

	300 mile	200 mile	250 mile	350 mile	400 mile
Travel Costs	-0.004***	-0.006***	-0.005***	-0.003***	-0.003***
	(0.000)	(0.000)	(0.000)	(0.000)	(0.000)
Secchi Depth	0.010***	0.015***	0.013***	0.009***	0.008***
	(0.002)	(0.002)	(0.002)	(0.002)	(0.002)
COVID	0.193***	0.205***	0.197***	0.192***	0.182***
	(0.010)	(0.010)	(0.010)	(0.009)	(0.009)
Secchi Depth X COVID	-0.000	0.001	0.000	-0.000	-0.001
	(0.001)	(0.001)	(0.001)	(0.001)	(0.001)
ln(Cumu. Cases)	-0.002***	-0.002***	-0.002***	-0.002***	-0.001***
	(0.000)	(0.000)	(0.000)	(0.000)	(0.000)
Lockdown Dummy	0.022***	0.025***	0.024***	0.020***	0.027***
	(0.007)	(0.008)	(0.008)	(0.007)	(0.007)
Observations	2819946	2613454	2723521	2890624	2948650
N(BlockGroup)	155145	145086	150051	156287	162831
CBG FEs	Yes	Yes	Yes	Yes	Yes
Site FEs	Yes	Yes	Yes	Yes	Yes
Weather FEs	Yes	Yes	Yes	Yes	Yes
MWTP	2.572	2.405	2.654	2.664	2.669

Notes: Table C3 shows the results of running the recreation demand model using alternative car-mode trip cutoffs. All specifications include site and CBG fixed effects, and weather controls. The standard error is clustered at the CBG level. Robust standard errors are in parentheses. ***,**,* denotes statistical significance at the 1%, 5%, and 10% levels, respectively. For additional details, see Section 4.

Table C4. Robustness Checks: Alternative Functional Forms

	(1)	(2)	(3)
Travel Costs	-0.004***	-0.004***	-0.004***
	(0.000)	(0.000)	(0.000)
COIVD	0.193***	0.193***	0.189***
	(0.010)	(0.010)	(0.010)
ln(Cumu. Cases)	-0.002***	-0.002***	-0.002***
	(0.000)	(0.000)	(0.000)
Lockdown Dummy	0.022***	0.022***	0.020***
	(0.007)	(0.007)	(0.007)
Secchi Depth	0.010***		
	(0.002)		
Secchi Depth X COVID	-0.000		
	(0.001)		
ln(Secchi Depth)		0.020***	
		(0.002)	
ln(Secchi Depth) X COVID		0.001	
		(0.001)	
Secchi Depth>2 m			0.021***
			(0.003)
Secchi Depth>2 m X COVID			0.021***
			(0.002)
Observations	2819946	2819946	2819946
N(BlockGroup)	155145	155145	155145
CBG FEs	Yes	Yes	Yes
Site FEs	Yes	Yes	Yes
Weather FEs	Yes	Yes	Yes

Notes: Table C4 shows the results of running the recreation demand model using water quality dummies or log form of water quality measures. All specifications include site and CBG fixed effects, and weather controls. the standard error is clustered at the CBG level. Robust standard errors are in parentheses. ***,**,* denotes statistical significance at the 1%, 5%, and 10% levels, respectively. For additional details, see Section 4.

Table C5. Robustness Checks: Prior Congestion Impacts

	(1)	(2)	(3)	(4)	(5)	(6)
Travel Costs	-0.004***	-0.004***	-0.004***	-0.004***	-0.004***	-0.004***
	(0.000)	(0.000)	(0.000)	(0.000)	(0.000)	(0.000)
Secchi Depth	0.012***	0.012***	0.010***	0.009***	0.014***	0.014***
	(0.002)	(0.002)	(0.002)	(0.002)	(0.002)	(0.002)
COVID	0.056***	0.057***	0.073***	0.072***	0.073***	0.074***
	(0.011)	(0.011)	(0.011)	(0.011)	(0.011)	(0.011)
Secchi Depth X COVID	0.002**	0.002**	0.002**	0.002**	0.000	-0.000
	(0.001)	(0.001)	(0.001)	(0.001)	(0.001)	(0.001)
ln(Cumu. Cases)	0.003***	0.003***	0.003***	0.003***	0.003***	0.003***
	(0.000)	(0.000)	(0.000)	(0.000)	(0.000)	(0.000)
Lockdown Dummy	0.060***	0.060***	0.044***	0.044***	0.046***	0.046***
	(0.008)	(0.008)	(0.008)	(0.008)	(0.008)	(0.008)
Observations	2122131	2122131	2122131	2122131	2122131	2122131
N(BlockGroup)	147142	147142	147142	147142	147142	147142
CBG FEs	Yes	Yes	Yes	Yes	Yes	Yes
Site FEs	Yes	Yes	Yes	Yes	Yes	Yes
Weather FEs	Yes	Yes	Yes	Yes	Yes	Yes
Prior Congestion	Lagged Relative Visits	Lagged Relative Visitors	Lagged Log of Visits	Lagged Log of Visitors	Lagged Visits	Lagged Visitors
MWTP	3.031	3.092	2.661	2.418	3.522	3.546

Notes: Table C5 shows the results of running the recreation demand model with prior congestion controls from 2019 to 2021. Lagged relative visits refer to the ratio of the number of visits at a site to the total number of visits from a CBG in the previous year. All specifications include site and CBG fixed effects, and weather controls. the standard error is clustered at the CBG level. Robust standard errors are in parentheses. ***,**,* denotes statistical significance at the 1%, 5%, and 10% levels, respectively. For additional details, see Section 4.

Table C6. Robustness Checks: Alternative Market Size

	(1)	(2)	(3)	(4)	(5)
Travel Costs	-0.004***	-0.004***	-0.004***	-0.004***	-0.004***
	(0.000)	(0.000)	(0.000)	(0.000)	(0.000)
Secchi Depth	0.010***	0.009***	0.009***	0.009***	0.009***
	(0.002)	(0.002)	(0.002)	(0.002)	(0.002)
COVID	0.193***	0.191***	0.190***	0.191***	0.190***
	(0.010)	(0.010)	(0.010)	(0.010)	(0.010)
Secchi Depth X COVID	-0.000	-0.000	-0.000	-0.000	-0.000
	(0.001)	(0.001)	(0.001)	(0.001)	(0.001)
ln(Cumu. Cases)	-0.002***	-0.002***	-0.002***	-0.002***	-0.002***
	(0.000)	(0.000)	(0.000)	(0.000)	(0.000)
Lockdown Dummy	0.022***	0.024***	0.025***	0.024***	0.025***
	(0.007)	(0.007)	(0.007)	(0.007)	(0.007)
Observations	2819946	2819946	2819946	2819946	2819946
N(BlockGroup)	155145	155145	155145	155145	155145
CBG FEs	Yes	Yes	Yes	Yes	Yes
Site FEs	Yes	Yes	Yes	Yes	Yes
Weather FEs	Yes	Yes	Yes	Yes	Yes
Market Size	115 days	190 days	365 days	115 days + 190 days for Univ.	115 days + 365 days for Univ.
MWTP	2.572	2.467	2.408	2.467	2.408

Notes: Table C6 shows the recreation demand results using alternative market sizes. Column 1 calculates the market size based on 115 days; column 2 calculates the market size based on 190 days; column 3 calculates the market size based on 365 days; column 4 calculates the market size based on 115 days for general CBGs and 190 days for CBGs adjacent to Universities; column 4 calculates the market size based on 115 days for general CBGs and 365 days for CBGs adjacent to Universities. The standard error is clustered at CBG level. Robust standard errors are in parentheses. ***,**,* denotes statistical significance at the 1%, 5%, and 10% levels, respectively. For additional details, see Section 4.

Table C7. Robustness Checks: Alternative Site Area and Visits Cutoffs

	(1)	(2)	(3)	(4)	(5)
Travel Costs	-0.004***	-0.004***	-0.004***	-0.004***	-0.004***
	(0.000)	(0.000)	(0.000)	(0.000)	(0.000)
Secchi Depth	0.010***	0.010***	0.010***	0.009***	0.008***
	(0.002)	(0.002)	(0.002)	(0.002)	(0.002)
COVID	0.187***	0.193***	0.194***	0.197***	0.197***
	(0.009)	(0.010)	(0.010)	(0.010)	(0.010)
Secchi Depth X COVID	0.000	-0.000	-0.000	-0.000	0.000
	(0.001)	(0.001)	(0.001)	(0.001)	(0.001)
ln(Cumu. Cases)	-0.001***	-0.002***	-0.002***	-0.002***	-0.002***
	(0.000)	(0.000)	(0.000)	(0.000)	(0.000)
Lockdown Dummy	0.022***	0.021***	0.022***	0.020***	0.024***
	(0.007)	(0.007)	(0.007)	(0.007)	(0.007)
Observations	2928580	2837537	2819946	2764191	2713401
N(BlockGroup)	156647	155561	155145	154915	154024
CBG FEs	Yes	Yes	Yes	Yes	Yes
Site FEs	Yes	Yes	Yes	Yes	Yes
Weather FEs	Yes	Yes	Yes	Yes	Yes
Year FEs	Yes	Yes	Yes	Yes	Yes
Area Size Lower Bound		1 Ha	1 Ha	2 Ha	2 Ha
Annual Visits Lower Bound			500		1000

Notes: Table C7 shows the recreation demand results using alternative cutoffs for site size and annual visits lower bound. Column 1 does not have any restrictions; column 2 only includes recreation sites with a site size above 1 Ha; column 3 only includes recreation sites in with a site size above 1 Ha and annual visits of more than 500; column 4 only includes recreation sites with a site size above 2 Ha; column 3 only includes recreation sites in with a site size above 2 Ha and annual visits of more than 1000. The standard error is clustered at CBG level. Robust standard errors are in parentheses. ***,**,* denotes statistical significance at the 1%, 5%, and 10% levels, respectively. For additional details, see Section 4.